THE INFLUENCE OF MYOBLAST IMPLANTATION ON ARTERIOGENESIS IN MICE WITH DIET-INDUCED OBESITY

A Senior Thesis

presented to the Faculty of California Polytechnic State University

San Luis Obispo

In Partial Fulfillment of the Requirements for the

Degree of Bachelor of Science in Biomedical Engineering

by

Rayana E. Gutierrez

May 2023

PROJECT INFORMATION

TITLE: The Influence of Myoblast Implantation on Arteriogenesis in Mice with Diet-Induced Obesity

AUTHOR: Rayana E. Gutierrez

DATE SUBMITTED: June 2023

ADVISOR: Trevor R. Cardinal, PhD
Professor of Biomedical Engineering

ABSTRACT

The Influence of Myoblast Implantation on Arteriogenesis
in Mice with Diet-Induced Obesity

Rayana E. Gutierrez

Peripheral arterial occlusive disease (PAOD) is characterized by atherosclerosis, which is the buildup of plaque, consisting largely of cholesterol, in the arterial walls. This plaque accumulation eventually blocks blood flow to the limbs, causing symptoms such as intermittent claudication and tissue death in cases of critical limb ischemia. The body compensates for the reduced perfusion by enlarging pre-existing bypass arteries, known as collaterals, in a process called arteriogenesis. However, in many cases, collateral networks constructed through arteriogenesis fail to enlarge sufficiently or function effectively in patients. Therefore, the development of a therapeutic intervention specifically targeting this process would offer a valuable solution for improving blood flow and facilitating tissue perfusion. Obesity and its comorbidities induce PAOD by promoting atherosclerosis, endothelial dysfunction, and impaired vascular function, so it is critical to analyze the degree of collateral remodeling following arteriogenesis in obese subjects to understand if the phenotype impacts the effectiveness of regenerative treatment. This study aims to determine whether myoblast implantation enhances collateral growth after induced ischemia in the hindlimbs of mice with diet-induced obesity (DIO) and in lean mice. PAOD was mimicked in all subjects by occluding blood flow in the femoral artery with a suture-based ligation. A thermally responsive, injectable polymer containing myoblasts, or no cells, was injected under the gracilis anterior, just deep to the targeted collateral. After 7 days post-operation, the polymer was removed and prepared for assessment. To assess the degree of collateral remodeling, perfusion fixation and vascular casting were performed, with subsequent removal of the anterior gracilis muscle for imaging and measuring vessel luminal/abluminal diameters and calculating arterial wall thickness. The analysis of the study revealed that there was no notable difference in collateral remodeling in the subjects that received the cell treatment and no difference in collateral diameters between the phenotypes (DIO and lean). However, the arterial wall thickness was larger in mice with DIO, regardless of the treatment received. Overall, the outcome of the experiment suggests that arteriogenesis was not enhanced by myoblast implantation in obese subjects.

Keywords: arteriogenesis, atherosclerosis, cell transplantation, collateral arteries, myoblasts

ACKNOWLEDGMENTS

I want to express a sincere thank you to Dr. Trevor Cardinal for providing me with guidance, expertise, and support throughout this research project and my journey as a student. Your invaluable knowledge and advice have played a crucial role in shaping my understanding of research approaches and in nurturing my passion for biomedical engineering.

I also want to extend my deepest appreciation to the dedicated students in the MaVR lab for their commitment, collaboration, and hard work that contributed to this project. Thank you, Nathan Tran, Tori Barrington, Ananya Goyal, Cole Burk, Erica Duffy, Lucas Lacambra, Sam Leingang, Simon Park, and Franklin Ng, for your help in providing cell polymer and performing microsurgeries and perfusion fixation/casting procedures. Working alongside such driven, inspiring, and compassionate individuals in the MaVR lab has been an incredible privilege. Some of my fondest memories of college revolve around the camaraderie we shared during those intense surgery weekends.

Lastly, I would like to give the biggest thanks to Mom, Dad, and my dearest friends for the support and encouragement that have been the driving force behind my pursuit of excellence. I hope to continue to make you all proud in the next chapter of my endeavors.

"Enthusiasm is common. Endurance is rare."

-Angela Duckworth

TABLE OF CONTENTS

Page

LIST OF FIGURES

Page

INTRODUCTION

Peripheral Arterial Occlusive Disease (PAOD) is a cardiovascular illness that affects over 200 million people worldwide, with 6.5 million being patients over the age of 40 in the United States [1, 2]. PAOD occurs due to atherosclerotic plaque build-up inside of the arteries, typically in the abdominal aorta, iliac, and femoral arteries. Risk factors include diabetes, dyslipidemia, hypertension, and smoking [1, 3]. Even in approximately half of the cases where individuals are asymptomatic, the presence of PAOD indicates systemic atherosclerosis and an elevated risk of heart disease and stroke [4]. In the early stages of atherosclerosis, the blood vessels adapt by dilating to optimize blood flow through the plaque-filled vessel [1]. However, once the vessels reach their dilation limit, the plaque continues to obstruct the arterial lumen, as seen in **Figure 1**, leading to reduced blood flow to the distal extremities and causing symptoms such as muscle pain, cramps, and fatigue [1,5]. If left untreated without revascularization, the risk of amputation within 6 months is 19%, which increases to 23% within 1 year [5]. Critical ischemic conditions resulting from PAOD lead to approximately 150,000 amputations in the United States [6]. Unfortunately, 20% of these amputations result in death within five years due to poor healing conditions [7].

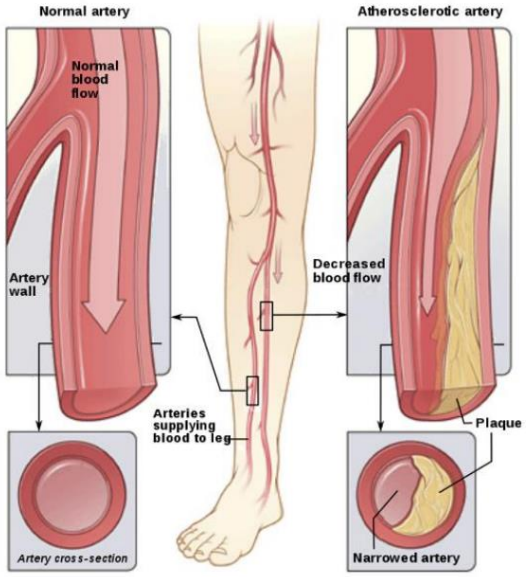

Figure 1. Blood flow in a healthy artery and in an atherosclerotic artery. PAOD entails the accumulation of plaque in the arteries, leading to inadequate blood flow and oxygen levels in the distal extremities [5].

The treatment options for patients with PAOD depend on the severity of their condition and associated symptoms. Exercise therapy is recommended for ambulatory patients to improve blood flow and slow disease progression [1]. Antiplatelet medications like acetylsalicylic acid (ASA), pentoxifylline, and cilostazol are prescribed to prevent blood clot formation, but their efficacy varies, and they may cause

adverse effects such as gastrointestinal bleeding and anemia. These drugs can also not be taken by patients with a history of congestive heart failure [1, 8]. In cases where physical or pharmaceutical therapies are ineffective, endovascular procedures like balloon angioplasties or stent placements are considered [7]. However, arterial restenosis, or narrowing of the vessels caused by smooth muscle cell proliferation in response to vessel damage, is a common complication after these interventions. Approximately 200,000 stents are placed in the femoral and popliteal arteries of PAOD patients each year?, and 30-40% of these cases experience in-stent restenosis within 2-3 years [9]. Furthermore, restenosis occurs in 60% of cases within 12 months following balloon angioplasty [7].

A potential solution to prevent amputation and reduce the need for surgical interventions lies in the enlargement of natural bypass arteries, emphasizing the importance of understanding the underlying mechanisms by which the body naturally facilitates this process. In response to an arterial occlusion, natural bypass collaterals undergo arteriogenesis, involving outward vascular remodeling in these vessels (**Figure 2**). More specifically, the obstruction caused by plaque buildup results in an elevated pressure gradient and shear stress between the proximal and distal arteries, leading to the enlargement of collateral vessels as they optimize blood flow to normalize shear forces [11]. At a cellular level, the endothelial cells lining the vessel lumen respond to increased shear stress by transducing the mechanical stimuli into intracellular activation of chemokines and adhesion molecules, which in induce the recruitment of monocytes [12].

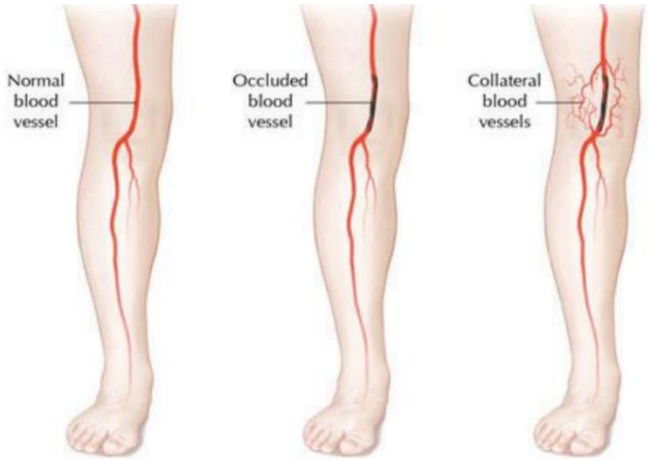

Figure 2. Collateral Vessels. Collaterals are natural bypass vessels that redirect blood around a blockage or obstruction in an artery, reinstating and normalizing the flow of blood to the surrounding and distal tissue [10].

These recruited monocytes differentiate into macrophages, which further enhance the inflammatory environment by secreting growth factors suchs as basic fibroblast growth factor (bFGF) and tumor necrosis factor-alpha (TNF-α). Moreover, macrophages produce matrix metalloproteinases, enzymes that degrade the elastic lamina and extracellular matrix (ECM) of the vessel. The combined effects of bFGF and TNF-α promote the proliferation of vascular smooth muscle cells (VSMCs), leading to the rearrangement and expansion of ECM components such as collagen and elastin. This remodeling process contributes to the enlargement of the internal elastic lamina and tunica media layers, resulting in a larger vessel size and enhanced perfusion to the distal tissues (**Figure 3**) [12] .

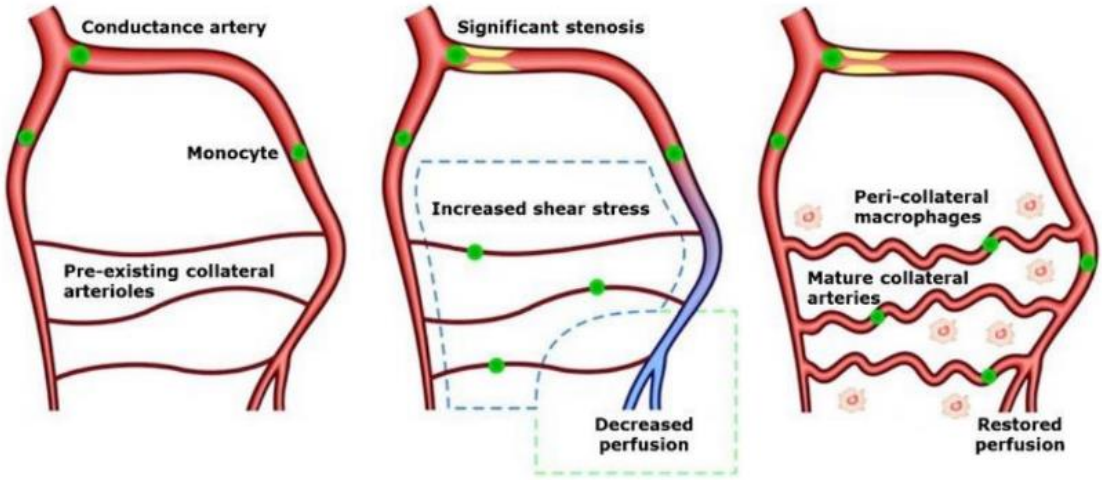

Figure 3. Macrophage-mediated Arteriogenesis. In unobstructed vasculature, blood flow is directed through the conductance artery (left). When the conductance artery is occluded, the increased shear stress is detected by the endothelium in the pre-existing collaterals, signaling for monocyte recruitment (middle). Monocytes differentiate into macrophages that induce cellular processes for arteriogenesis, ultimately restoring adequate perfusion (right) [13].

Although various regenerative solutions, including gene, protein, and cell-based therapies, have been tested in clinical trials for their efficacy in treating PAOD, only a few trials have successfully demonstrated increased arteriogenesis in humans compared to preclinical animal trials [14]. Examples of therapeutic products studied include bFGF protein, VEGF gene-plasmid, bone marrow-derived mononuclear cells (BMMNCs), peripheral blood-derived cells, and mesenchymal stem cells [14, 15]. The outcomes of these therapeutic treatments in human trials have been criticized for their uncontrolled nature

and small sample sizes, whereas larger randomized clinical trials have failed to replicate the positive results achieved in smaller studies [14]. Conversely, animal studies consistently demonstrate successful enhancement of arteriogenesis, including murine and rabbit hindlimb models with induced arterial occlusion and monocyte implantation [16, 17]. The reasons for the disparities between human and animal trial outcomes remain uncertain, but it is likely that challenges in managing physiological variability contribute to these differences [14].

It is important to recognize that obesity, frequently observed in patients with PAOD, is due to excessive fat accumulation and triggers oxidative stress, insulin resistance, inflammation, and ultimately, endothelial dysfunction [18]. Since obesity has a significant impact on arterial remodeling, it becomes crucial to replicate these physiological characteristics in animal models during preclinical studies. There is a correlation between obesity and lower circulating levels of endothelial progenitor cells (EPCs), which are cells that contribute to vascular repair and regeneration through direct and paracrine mechanisms [19]. The diminished presence of EPCs in the blood may lower the efficiency of arteriogenesis and reduce endothelial function in collaterals in the cases of PAOD in obese patients. Due to the scarcity of clinical trials substantiating the efficacy of EPC injection and other cell-based therapies (such as bFGF protein, BMMNCs, and mesenchymal stem cells) in the treatment PAOD, it is crucial to explore alternative promising treatments such as myoblast implantation.

Myoblasts, a type of progenitor cell found in skeletal muscle that is responsible for the regeneration of muscle fibers, have been thoroughly observed in the applications of stem cell therapy, gene therapy, and tissue engineering [20]. Upon activation in response to muscle fiber injury, satellite cells undergo proliferation and differentiation into myoblasts, and eventual maturation into myocytes and myotubes to generate new muscle fibers, thereby aiding in the repair and regeneration of damaged muscle tissue [21]. As previously mentioned, macrophages play a vital role in regulating arteriogenesis, and although the connection is not fully understood, researchers have noted that activated myoblasts may be positively influenced by the presence of macrophages [22]. The possible interaction between skeletal muscle

progenitor cells and macrophages amplifies the significance of investigating myoblasts as essential components for enhancing arteriogenesis. A previous study has shown that implanted myoblasts seeded onto gelatin constructs into mice with diet-induced obesity (DIO), following femoral artery ligation, improved arteriogenesis and enhanced functional vasodilation [23]. Building upon this research, the study discussed in this paper aimed to replicate the previous work, by use of a clinically applicable cell delivery construct which consists of a thermally responsive, injectable polymer that remains in liquid form inside a syringe until exposed to the body temperature of approximately 37°C. Injecting the cell vehicle may prove to be safer and more efficient to use in future clinical cases relative to the gelatin construct utilized in the previous study. The hypothesis of this experiment is that myoblasts injected under the gracilis muscles following femoral artery ligation, will enhance arteriogenesis within the collaterals in mice with DIO, assessed at 7 days after the operation.

METHODS

Animals

Every animal procedure involved in this study was approved by the Institutional Animal Care and Use Committee (IACUC) of California Polytechnic State University. The subjects consisted of 17–20-week-old C57BL/6 male mice (n=22) that were received from The Jackson Laboratory. Upon delivery to the university vivarium, the mice were housed in groups of 4-6, in cages with ad libitum access to food and water. The vivarium room was consistently regulated for temperature and lighting conditions, following a 12-hour light and dark cycle. The conditions of the mice, feed, water, and room were inspected daily. Following their arrival at the facility, the mice continued their specialized diet of either control feed (10% fat) for lean mice (n=5), or treatment feed (60% fat) for mice with DIO (n=17). The subjects were acclimated to the housing environments approximately two weeks prior to the first surgery. Following a survival procedure, the mice were reintroduced to the vivarium and placed in pairs, each with their designated food, until the 7-day assessment period.

Femoral Artery Ligation

To replicate the ischemic conditions associated with PAOD, a suture-based ligation was performed on the hindlimb of each subject. The ligation site was specifically targeted at the femoral artery, chosen as the region upstream (proximal) to the saphenous and popliteal arteries, and downstream (distal) from the epigastric and profunda arteries. Mice were first anesthetized in an induction chamber using a mixture of 5% isoflurane in oxygen, with a flow rate ranging from 0.8 to 1.6 $L \cdot min^{-1}$. Once adequately anesthetized, the mice were weighed and transferred to the preparation stage, where they were positioned in a supine orientation while receiving 1.5-2.5% isoflurane mixed with oxygen delivered through a 'nose-cone'. On the preparation bench, veterinary ophthalmic ointment was applied to the eyes to prevent corneal desiccation and depilatory cream was used to remove the hair from the surgical area on the medial aspect of both hindlimbs. Before placing the mouse on the surgical stage, a preoperative analgesic of buprenorphine (0.075 $mg \cdot kg^{-1}$) was administered subcutaneously via injection. To maintain the body temperature of the mice at 35°C, a temperature-controlled heat pad, and a thermal rectal probe. All surgical instruments were autoclaved prior, and aseptic technique was maintained throughout the entirety of the surgical procedure to prevent contamination and wound infection.

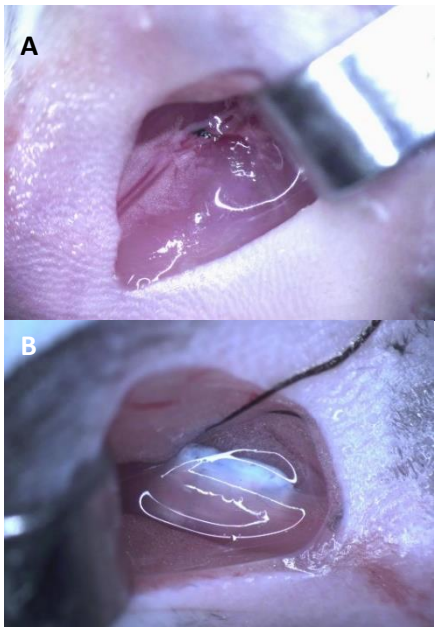

Figure 4. Femoral Artery Ligation and Implantation. Ligation tied at femoral artery 6.0 silk suture (A) followed by injection of thermally responsive polymer underneath the gracilis muscle (B).

Within the neurovascular bundle, the femoral artery was separated from the adjacent vein and nerve before ligating the vessel with 6.0 silk suture (**Figure 4A**). A thermally responsive polymer with myoblasts (n=11, 2 lean and 9 DIO subjects) was injected underneath the gracilis muscle of the operated hindlimb (**Figure 4B**). The non-treated subjects were given cell-free polymer vehicles (n=11, 3 lean and 8 DIO subjects),. After implantation, the skin incision was closed using 7-0 polypropylene suture. As the control, a sham surgery

was performed on the contralateral limb of each subject except for the neurovascular separation, femoral artery ligation, and polymer implantation. Buprenorphine was administered immediately post-operation ($0.075\ mg \cdot kg^{-1}$), and the subject was contained in a recovery bin until ambulatory. Analgesic was given for two consecutive days after the day of operation.

Perfusion Fixation and Vascular Casting

Perfusion fixation and vascular casting were performed to prepare for immunofluorescent staining and imaging of the gracilis muscle collateral. First, a thoracotomy was done to achieve access to the heart, which was then cannulated using a 23G needle in the left ventricle. An incision in the right atrium of the heart was made prior to injecting 25ml of the vasodilator cocktail heated to 37 °C ($5\ U \cdot \mu L^{-1}$ heparin, 10^{-4} M sodium nitroprusside, 10^{-4} M adenosine, in phosphate buffer solution (PBS)) at about 5ml/min, followed by 4% paraformaldehyde injected at a pressure of 90-110 mmHg. Next, vascular casting was completed by injecting a microfilament solution at a rate of 0.5-0.9 ml/min using a syringe pump until the casting spanned the anterior gracilis collaterals **(Figure 5**).

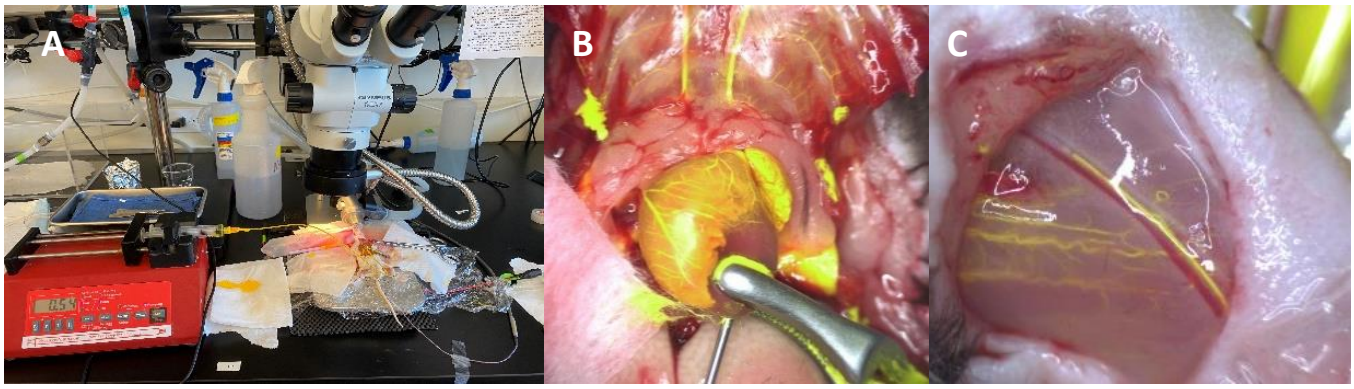

Figure 5. Vascular Casting. The casting set-up entails the use of a syringe pump to inject the microfilament solution **(A)** into the subject's system through a cannula placed in the pre-existing hole in the left ventricle **(B)**. The infusion is stopped once the solution spreads through the gracilis anterior collateral **(C)**.

Once the solution surpassed the knee joint in the saphenous artery, a makeshift tourniquet, using 2.0 silk suture, was tied around the ankle to prevent the microfilament from entering the veins through the ankle A-V shunts. To allow time for the microfilament to cure, the subjects were left overnight at room temperature, and the gracilis muscles from the operated and sham hindlimbs were resected the following day. The anterior gracilis and the adjacent saphenous artery were stored in a microcentrifuge tube with PBS at 4°C before immunofluorescent staining.

Immunofluorescence and Microscopy

Immunofluorescence staining was carried out to visualize the smooth muscle surrounding the collateral. The gracilis anterior muscles were stained with α-smooth muscle actin (ASMA) in a solution containing 2% bovine serum albumin (BSA) and 0.1% Triton in PBS for approximately 72 hours at 4°C. After the staining period, the muscles were rinsed in 0.1% Triton in PBS three times for 10 minutes, in addition to a PBS rinse for 30 minutes at room temperature.

Images of the collaterals were obtained through an inverted widefield microscope, in parallel with the Infinity Capture imagining software. A fluorescence setting (Cy3 excitation: 550 nm, emission 570 nm) on the microscope was used to view and take photos of the ASMA stain at a 4X and 10X objective. The brightfield setting on the same microscope was set to observe the microfilament casting in the collateral lumen, and an image was captured at a 10X objective.

Data Collection and Analysis

All diameter measurements were taken from the 10X images using the line measuring tool in ImageJ software. The measurement scale was calibrated at 10X prior to taking the data of the collaterals. Measurements were taken at the midzone in three locations along the collateral. Outer (abluminal) vessel diameter was taken from the collateral width on the ASMA fluorescent images, the inner (luminal) vessel diameter was taken from the collateral width along the same zone on the vascular casting images. The arterial wall thickness was calculated from the inner and outer diameter measurements.

Differences in the inner and outer diameters, and collateral wall thicknesses among the various groups were determined through a two-way ANOVA and Tukey Post-Hoc comparisons. All values are expressed as mean ± standard error.

RESULTS

The aim of this study was to develop a regenerative cell therapy for inducing natural bypass enlargement in patients with atherosclerotic arteries, a common occurrence in PAOD. To achieve this, ischemic conditions were created in the subjects by performing femoral artery ligation surgery (n=22), followed by the implantation of a thermally responsive, injectable polymer with (n=11) or without (n=11) myoblasts . After 7 days post-surgery, perfusion fixation and vascular casting techniques were employed to allow measurement of collateral diameters post with fluorescence and brightfield microscopy. In summary, myoblasts did not enhance the enlargement of collaterals in the gracilis anterior muscles (**Figures 6-8)**.

Myoblasts did not impact the luminal diameters of the collaterals in the anterior gracilis (**Figure 6**). There was no significant difference in the inner diameter on the operated hindlimb that received myoblasts between phenotypes (lean: 65.0 ± 3.12μm, DIO: 66.7 ± 10.3μm), or between the operated hindlimbs that received the control vehicle (lean: 67.3 ± 21.5, DIO: 74.23 ± 4.94μm, respectively).

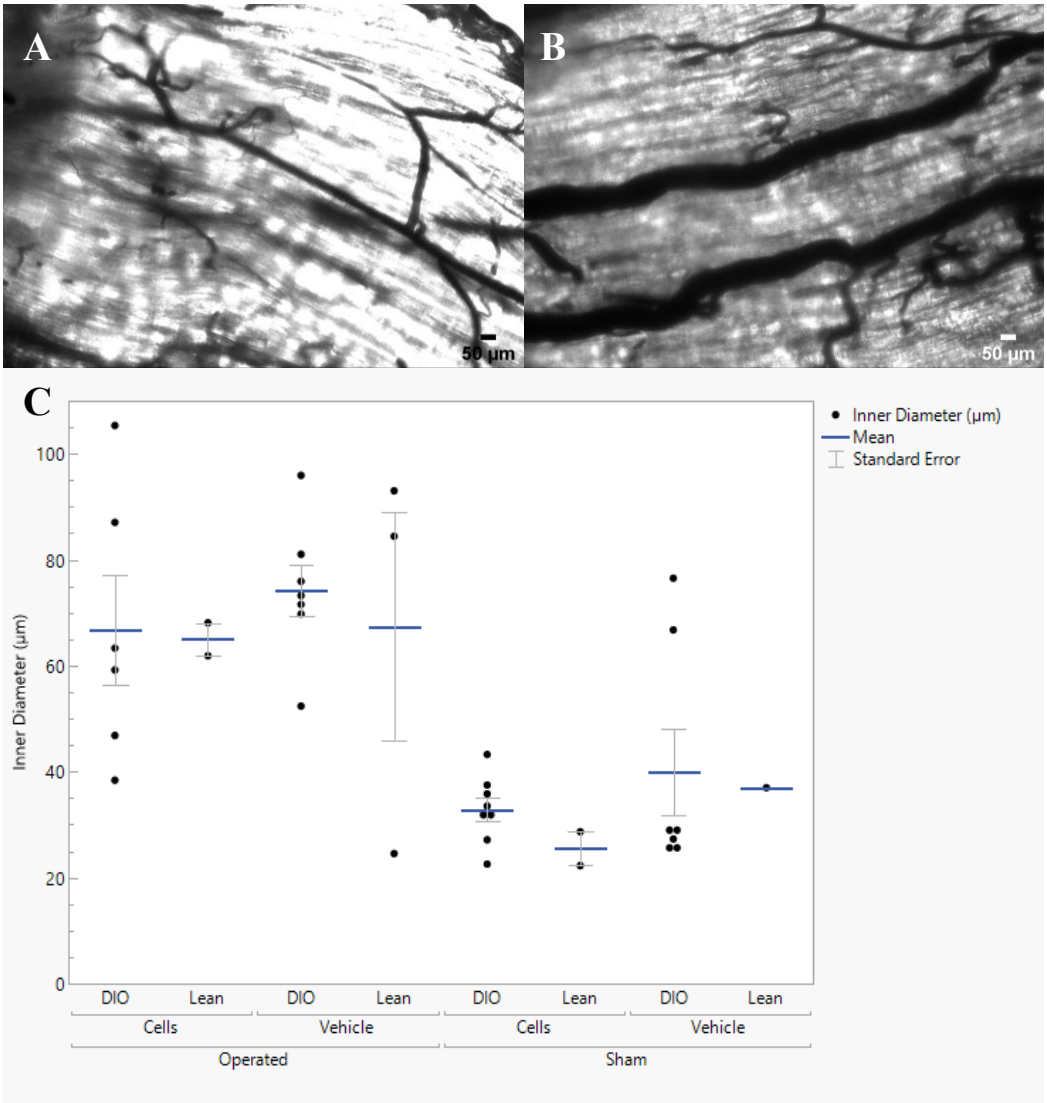

Figure 6. Luminal Diameter of Anterior Gracilis Collateral 7 Days Post-Artery Ligation and Implantation. **(A)** Representative day-7 post ligation collateral luminal diameter Microfilament casted in sham hindlimb (10x). **(B)** Representative day-7 post ligation collateral luminal-diameter Microfilament casted in operated hindlimb (10x). **(C)** The inner diameters (µm) of anterior gracilis collaterals in day-7 post-ligation hindlimbs in DIO w/cell treatment, lean w/ cells, DIO w/o cells, and lean w/o cells (n=6, 2, 7, 3)* and the control hindlimbs (sham) in DIO w/cell treatment, lean w/cells, DIO w/o cells, and lean w/o cells (n=8, 2, 7, 1)* (all C57Bl/6 male mice). No differences were detected between the inner diameters of DIO and lean subjects or between mice that received the myoblasts or vehicle transplant. (*n represents the number of hindlimbs, not subjects).

Likewise, myoblasts did not affect the abluminal diameters of the collaterals **(Figure 7)**, as the outer diameters in the operated hindlimb with the treatment (lean: 72.84 ± 4.85µm, DIO: 66 ± 11.2µm) were not significantly different then in operated limbs with the control vehicle (lean: 76.8 ± 18., DIO: 81.77 ± 7.35 µm, respectively).

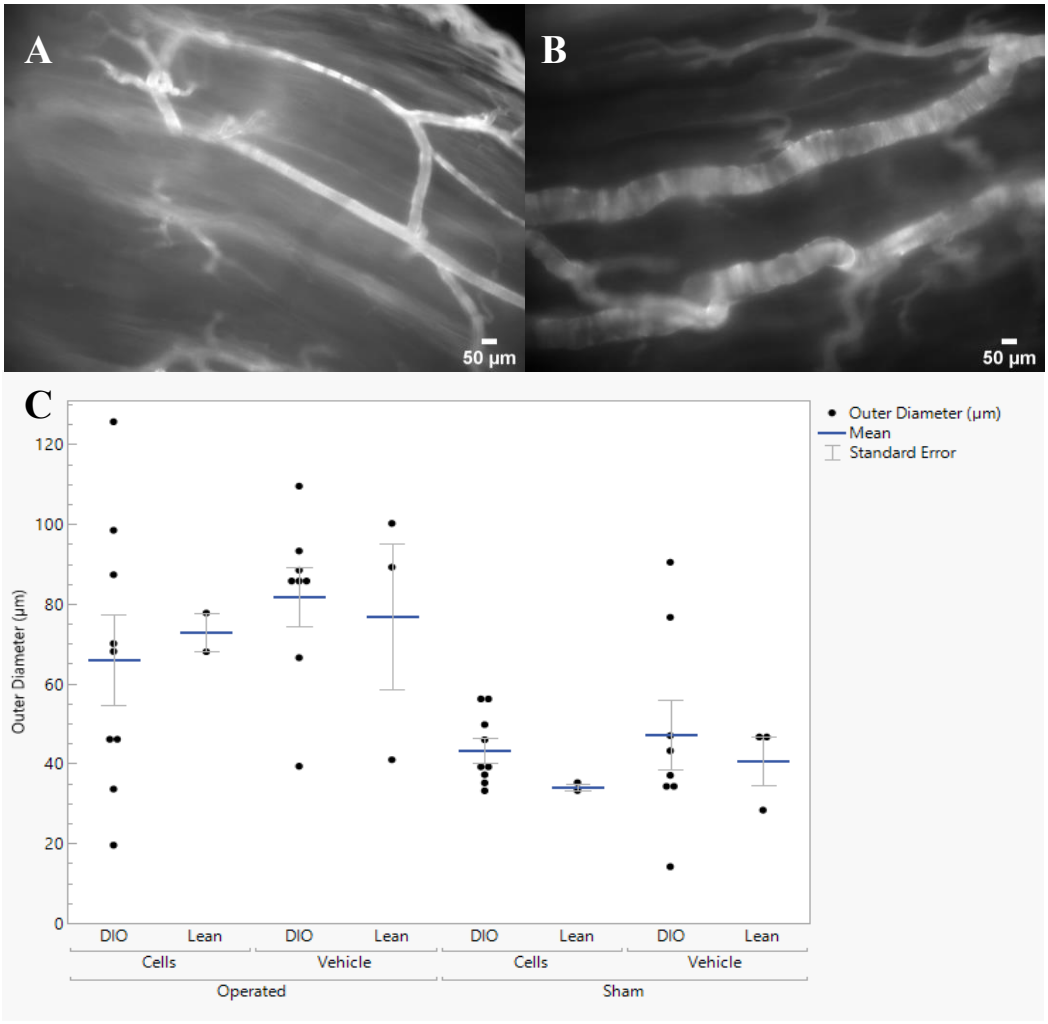

Figure 7. Abluminal Diameter of Anterior Gracilis Collateral 7 Days Post-Artery Ligation and Implantation. (A) Representative day-7 post ligation collateral abluminal diameter ASMA stained in sham hindlimb (10x). **(B)** Representative day-7 post ligation collateral abluminal-diameter ASMA stained in operated hindlimb (10x). **(C)** The outer diameters (µm) of anterior gracilis collaterals in day-7 post-ligation hindlimbs in DIO w/cell treatment, lean w/cells, DIO w/o cells, and lean w/o cells (n = 9, 2, 8, 3)* and the control hindlimbs (sham) in DIO w/cell treatment, lean w/cells, DIO w/o cells, and lean w/o cells (n = 8, 2, 8, 3)* (all C57Bl/6 male mice). No differences were detected between the outer diameters of DIO and lean subjects or between mice that received the myoblasts or vehicle transplant. (*n represents the number of

Although the myoblasts did not impact the collateral wall thickness in the operated hindlimb (lean: 7.84 ± 1.73µm, DIO: 15.88 ± 2.89 µm) as the measurements were similar to the subjects that received the vehicle (lean: 9.42 ± 3.55, DIO: 13.60 ± 1.99 µm, respectively), the wall thickness was larger in mice with DIO than in lean mice ($p<0.05$) (**Figure 8**).

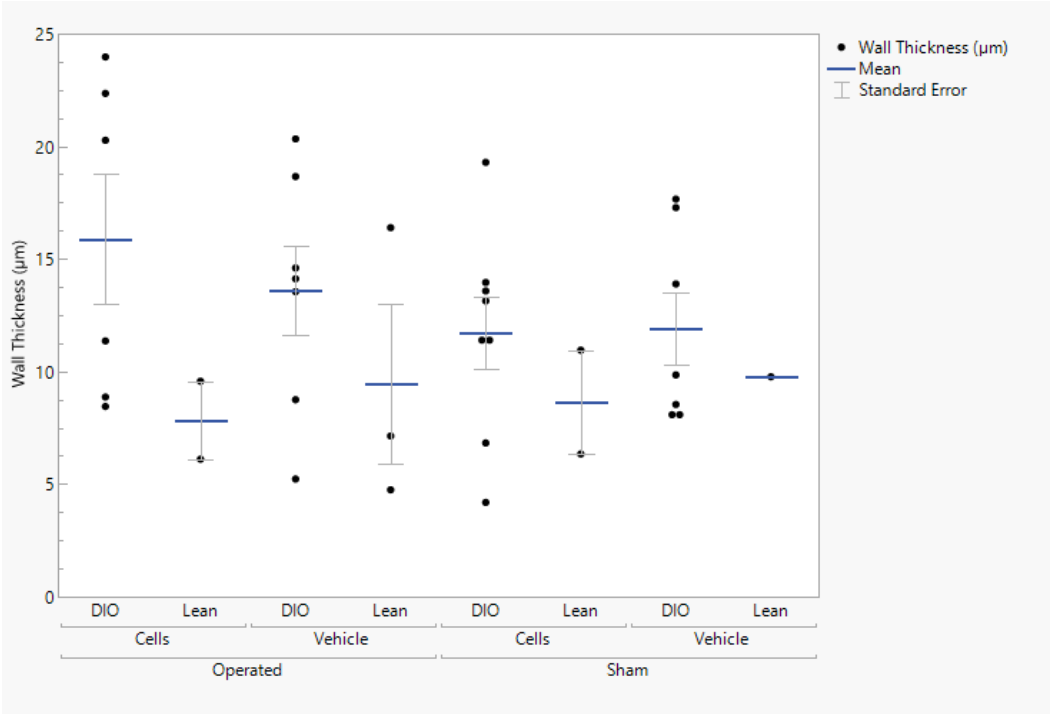

Figure 8. Wall Thickness of Anterior Gracilis Collateral 7 Days Post-Artery Ligation and Implantation. The arterial wall thickness (µm) of anterior gracilis collaterals in day-7 post-ligation hindlimbs in DIO w/cell treatment, lean w/ cells, DIO w/o cells, and lean w/o cells (n=6, 2, 7, 3)* and the control hindlimbs (sham) in DIO w/cell treatment, lean w/cells, DIO w/o cells, and lean w/o cells (n=8, 2, 7, 1)* (all C57Bl/6 male mice). The statistical analysis demonstrates that the wall thickness in DIO subjects is greater than in lean subjects ($p<0.05$). However, there is no difference in arterial wall thickness between subjects that received the cell treatment and those that received the vehicle. (*n represents the number of hindlimbs, not subjects).

DISCUSSION

Peripheral Arterial Occlusive Disease (PAOD) affects around 8-12 million individuals [24]. This condition arises when excessive cholesterol in the bloodstream accumulate as plaque in the arteries, leading to a reduction in blood flow to the limbs or other distant organs. While about 50% of people with this condition do not experience any symptoms, the disease can result in claudication and progress to a stage known as critical limb ischemia, which significantly increases the risk of limb amputation. In response to the mechanical pressures and stresses caused by arterial occlusion, the natural bypass arteries can enlarge through a process called arteriogenesis, which helps increase blood flow to the areas of

reduced perfusion. This study aimed to explore the potential of cell therapy, specifically the use of muscle progenitor cells known as myoblasts, to enhance the arteriogenesis process in cases of PAOD and analyze the treatment's effects on obese subjects. Mice with DIO and lean mice were surgically modified to mimic ischemic conditions found in patients of PAOD, and other in-vivo surgical procedures were utilized to investigate the effects of myoblast transplantation on arteriogenesis.

The data from this study concludes that myoblasts did not enhance nor impair arteriogenesis. In contrast to the previous study that utilized a gelatin vehicle and demonstrated significant outcomes with myoblast implantation, the present experiment employed a N-isopropylacrylamide (NIPAM) based polymer, which has shown to be a biocompatible vehicle for myoblasts [25]. In the NIPAM construct, the cells were dispersed throughout the material, while in the gelatin construct, the cells were primarily located on the top layer that was in direct contact with the gracilis upon implantation [23]. Therefore, one plausible theory for the non-replication of results in this study could be that an adequate number of myoblasts in the NIPAM vehicle could not migrate sufficiently close to the collaterals to induce a local response. Further investigations involving cell tracking in the polymer and local muscle fibers on the 7-day assessment are necessary to ascertain the impact of cell placement and migration within the polymer on collateral remodeling.

Mouse phenotype, i.e., diet induced obesity or lean did not impact the abluminal and luminal diameters of the anterior gracilis collaterals. As expected, there was greater collateral remodeling in the operated hindlimbs compared to the sham hindlimbs (Appendix I), ensuring that the femoral artery ligation was overall effective in mimicking the ischemic conditions found in patients with PAOD.

Although myoblast treatment had no effect, it was evident that the wall thickness in the subjects with DIO was larger than that in the lean subjects. A greater intima-media thickness has been repeatedly observed in the carotid arteries in obese humans, and a few studies even suggest that body weight has a greater impact on the arterial thickness relative to lumen diameter [26-28]. A greater wall thickness is indicative of vascular smooth muscle cell (VSMC) hypertrophy, which occurs in response to arterial

injury and remodeling, such as in cases of atherosclerosis [29]. This hypertrophic response is influenced by the interaction of VSMCs with endothelial cells, inflammatory cells, and a variety of growth factors. Patients with obese phenotypes often exhibit elevated levels of perivascular adipose tissue (PVAT), which directly surrounds blood vessels and exerts local effects on vascular function [30]. Growth factors released from the perivascular fat can regulate VSMC proliferation and migration from the tunica media to intima, leading to overall hypertrophic changes. Adipokines, including Visfatin, which are cytokines released by PVAT, partially induce VSMC hypertrophy through paracrine signaling and adipocyte-conditioned media containing Visfatin derived from human adipocytes can increase the human VSMCs proliferation [30]. Moreover, PVAT adipocytes express and secrete significant amounts of growth factors such as thrombospondin-1, vascular endothelial growth factor (VEGF), and basic fibroblast growth factor (bFGF), which stimulate VSMC proliferation and migration [31]. Even though a majority of PVAT is located around arteries, large veins, and arterioles it can also be found within the vascular walls of small vessels located within striated muscle [32, 33]. If the mice with DIO in this study had higher levels of PVAT within the collateral vessels, the increased presence of adipokines and PVAT-derived growth factors could potentially explain the notable increase in wall thickness observed in the obese subjects.

The study encountered several limitations that should be taken into consideration. Firstly, it is important to note that the vascular casting procedure encountered difficulties in nine hindlimbs (two in the lean group and seven in the DIO group). The protocol failed in these subjects as the Microfilament solution did not reach the targeted collaterals, hence a luminal diameter measurement could not be obtained. Another limitation that may have affected the accuracy of the data is the blurriness observed in some of the ASMA fluorescent collateral images. In certain samples, the position of the collateral in relation to the surrounding muscles made it challenging to obtain a clearly defined outer diameter edge, thus posing difficulties in accurate measurement taking using ImageJ. The lack of well-defined edges could have introduced variability and potential measurement errors, which should be taken into consideration when interpreting the results.

Future studies should prioritize identifying the factors contributing to the failure of the vascular casting procedure to significantly improve the consistency and reliability of luminal diameter measurements. Perhaps preparing the stained muscle in a way that allows for clear capturing of images at 40X objective, as opposed to 10X, will yield to more precise data. Furthermore, to reduce variability, future studies should focus on maintaining a singular phenotype during the investigation by selecting either all lean or mice with DIO for studying the arteriogenic response to femoral artery ligation. The present study had a small sample size of only 5 lean mice compared to 17 mice with DIO. This discrepancy in sample sizes may have made it challenging to make a fair comparison between the outcomes of the two phenotypes, and instead, introduced unnecessary variability.

Given that the significant differences observed in this study were primarily related to wall thickness variations among phenotypes, it would be worthwhile to conduct a research study that measures collateral remodeling in both mice with DIO and lean mice without the myoblast transplantation. This approach would provide a clearer examination of the natural biochemical differences that occur, and such research could supplement our understanding of how regenerative solutions can enhance the arteriogenic response in both patient phenotypes.

CONCLUSION

The study findings demonstrated that myoblasts did not enhance arteriogenesis in mice with DIO. However, an interesting observation was made regarding the larger wall thickness of the collateral vessels in the obese subjects. This suggests the involvement of significant paracrine signaling of growth factors and cellular processes triggered by arterial occlusion, that are possibly present in greater quantities in obese individuals. To gain a deeper understanding of the myoblast treatment on arteriogenesis, further analysis should focus on studying it in a more balanced manner, either within a single phenotype or by ensuring a more equitable distribution of obese and lean subjects. The continued advancement of regenerative therapies offers the potential to provide alternative and minimally invasive treatments that

can alleviate symptoms and improve overall patient outcomes. By harnessing the power of regenerative medicine, researchers can make significant strides in improving the lives of individuals affected by vascular diseases, including PAOD.

REFERENCES

[1] Zemaitis, M. R., Boll, J. M., & Dreyer, M. A. (2023, May 23). Peripheral Arterial Disease. R. A. Brown & P. D. Barker (Eds.), *StatPearls*.

[2] Centers for Disease Control and Prevention. (n.d.). Peripheral Arterial Disease (PAD). Retrieved fromhttps://www.cdc.gov/heartdisease/PAD.htm

[3] Medical Advisory Secretariat. (2010). Stenting for peripheral artery disease of the lower extremities: an evidence-based analysis. *Ont Health Technol Assess Ser*, 10(18), 1-88.

[4] Topfer, L. A., & Spry, C. (2018, April 1). New Technologies for the Treatment of Peripheral Artery Disease. In *CADTH Issues in Emerging Health Technologies*. Canadian Agency for Drugs and Technologies in Health; 2016-. (Issue 172).

[5] National Heart, Lung, and Blood Institute. (n.d.). Causes of Peripheral Artery Disease. Retrieved from https://www.nhlbi.nih.gov/health/peripheral-artery-disease/causes

[6] Coastal Vascular & Interventional, PLLC. (n.d.). Leg Amputation Can Be Avoided in PAD Patients. Retrieved from https://coastalvascular.net/leg-amputation-can-avoided-pad-patients/

[7] USA Vascular Centers. (n.d.). Can Peripheral Artery Disease Lead to Death? Retrieved from https://www.usavascularcenters.com/blog/can-peripheral-artery-disease-lead-to-death/

[8] Schmit, K., Dolor, R. J., Jones, W. S., Vemulapalli, S., Hasselblad, V., Subherwal, S., Heidenfelder, B., & Patel, M. R. (2014, December 4). Comparative effectiveness review of antiplatelet agents in peripheral artery disease. *Journal of the American Heart Association, 3*(6).

[9] Lichtenberg, M. K., Carr, J. G., & Golzar, J. A. (2017, August). Optical coherence tomography: guided therapy of in-stent restenosis for peripheral arterial disease. *Journal of Cardiovascular Surgery (Torino), 58*(4), 518-527.

[10] Peripheral Arterial Disease. (2014, October 16). *Redbacteria.* Retrieved from https://redbacteria.wordpress.com/2014/10/06/

[11] Ma, T., & Bai, Y. P. (2020, March 16). The hydromechanics in arteriogenesis. *Aging Medicine (Milton), 3*(3), 169-177.

[12] Shahzad, K., Bock, F., Dong, W., Wang, H., Kopf, S., Kohli, S., ... & Sindrilaru, A. (2013). The IL-23/IL-17 axis orchestrates the immune response to ovarian cancer in preclinical models. *Journal of Leukocyte Biology, 93*(6), 825-832.

[13] Hendrikx, G., Vöö, S., Bauwens, M., Post, M. J., & Mottaghy, F. M. (2016, December). SPECT and PET imaging of angiogenesis and arteriogenesis in pre-clinical models of myocardial ischemia and peripheral vascular disease. *European Journal of Nuclear Medicine and Molecular Imaging, 43*(13), 2433-2447.

[14] Botham, C. M., Bennett, W. L., & Cooke, J. P. (2013, October-December). Clinical trials of adult stem cell therapy for peripheral artery disease. *Methodist DeBakey Cardiovascular Journal, 9*(4), 201-205.

[15] Gorski, D. H., Beilhack, G. F., Merrilees, M. J., & Sanders, J. M. (2021). Current Insights Into the Role of Proteoglycans in Vascular Biology. *Arteriosclerosis, Thrombosis, and Vascular Biology, 41*(2), 556-572.

[16] Arras, M., Ito, W. D., Scholz, D., Winkler, B., Schaper, J., & Schaper, W. (1998, January 1). Monocyte activation in angiogenesis and collateral growth in the rabbit hindlimb. *Journal of Clinical Investigation, 101*(1), 40-50.

[17] Francke, A., et al. (2013). Transplantation of bone marrow derived monocytes: a novel approach for augmentation of arteriogenesis in a murine model of femoral artery ligation. *American Journal of Translational Research, 5*(2), 155-169.

[18] Stapleton, P. A., James, M. E., Goodwill, A. G., & Frisbee, J. C. (2008, August). Obesity and vascular dysfunction. *Pathophysiology, 15*(2), 79-89.

[19] Tsai, T. H., Chai, H. T., Sun, C. K., Yen, C. H., Leu, S., Chen, Y. L., ... Yip, H. K. (2012, July 2). Obesity suppresses circulating level and function of endothelial progenitor cells and heart function. *Journal of Translational Medicine, 10*, 137.

[20] Yu, D., et al. (2021, February 4). Myogenic Differentiation of Stem Cells for Skeletal Muscle Regeneration. *Stem Cells International, 2021*, 8884283.

[21] Kim, J. H., Jin, P., Duan, R., & Chen, E. H. (2015, June). Mechanisms of myoblast fusion during muscle development. *Current Opinion in Genetics & Development, 32*, 162-170.

[22] Pajcini, K. V., et al. (2008, March 10). Myoblasts and macrophages share molecular components that contribute to cell-cell fusion. *Journal of Cell Biology, 180*(5), 1005-1019.

[23] Tran, C. M., Hamzeinejad, V., & Cardinal, T. R. (2018). The Impact of Primary Myoblast Transplantation on Functional Vasodilation Following Arteriogenesis in Mice with Diet-Induced Obesity. *The FASEB Journal, 32*(S1), 573.10-573.10.

[24] U.S. Department of Health and Human Services. (August 2006). Facts About Peripheral Arterial Disease (P.A.D.). NIH Publication No. 06-5837.

[25] Klueter, Q. R. (2022). Optimization Of A Novel Nipam-Based Thermoresponsive Copolymer For Intramuscular Injection As A Myoblast Delivery Vehicle To Combat Peripheral Artery Occlusive Disease. Available at: https://digitalcommons.calpoly.edu/theses/2565.

[26] Kotsis, V. T., Stabouli, S. V., Papamichael, C. M., & Zakopoulos, N. A. (2006). Impact of obesity in intima media thickness of carotid arteries. Obesity (Silver Spring), 14(10), 1708-1715.

[27] De Michele, M., et. al. (2002). Association of obesity and central fat distribution with carotid artery wall thickening in middle-aged women. *Stroke*, 33, 2923-2928.

[28] Kappus, R. M., et.al. (2014). Obesity and overweight associated with increased carotid diameter and decreased arterial function in young otherwise healthy men. *American Journal of Hypertension*, 27(4), 628-634.

[29] Berk, B. C. (2001). Vascular smooth muscle growth: Autocrine growth mechanisms. *Physiological Reviews*, 81(3), 999-1030.

[30] Miao, C. Y., & Li, Z. Y. (2012). The role of perivascular adipose tissue in vascular smooth muscle cell growth. *British Journal of Pharmacology*, 165(3), 643-658.

[31] Chang, L., Garcia-Barrio, M. T., & Chen, Y. E. (2020). Perivascular adipose tissue regulates vascular function by targeting vascular smooth muscle cells. *Arteriosclerosis, Thrombosis, and Vascular Biology*, 40(5), 1094-1109.

[32] Grigoras, A., et al. (2019). Perivascular adipose tissue in cardiovascular diseases-an update. *Anatol J Cardiol*, 22(5), 219-231.

[33] Gil-Ortega, M., et al. (2015). Regional differences in perivascular adipose tissue impacting vascular homeostasis. *Trends Endocrinol Metab*, 26(7), 367-375.

APPENDICIES

Appendix A: Raw Images

(Absence of Microfilament images indicates that the Micofil solution did not enter the collateral during casting procedure.)

Replicate N1: Lean, Cell

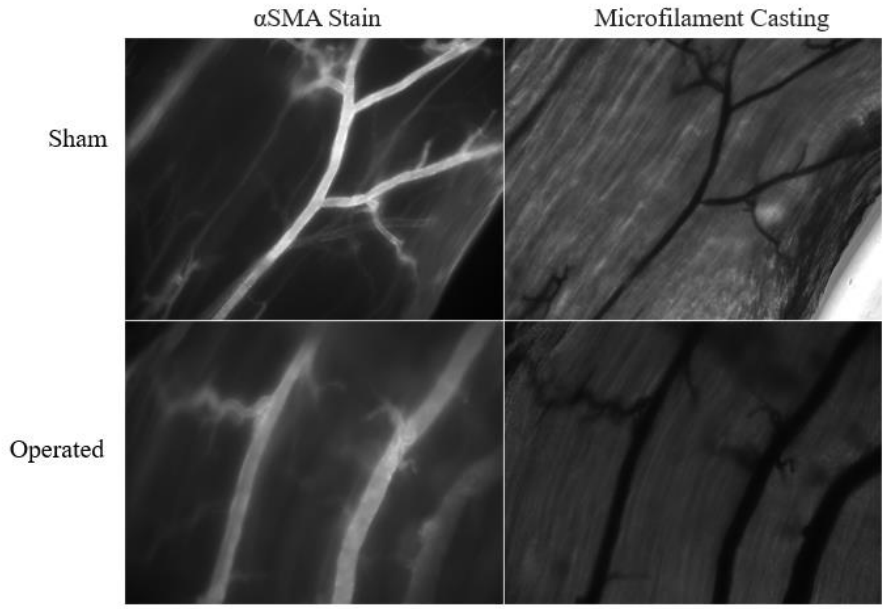

Replicate N1: DIO, Cell

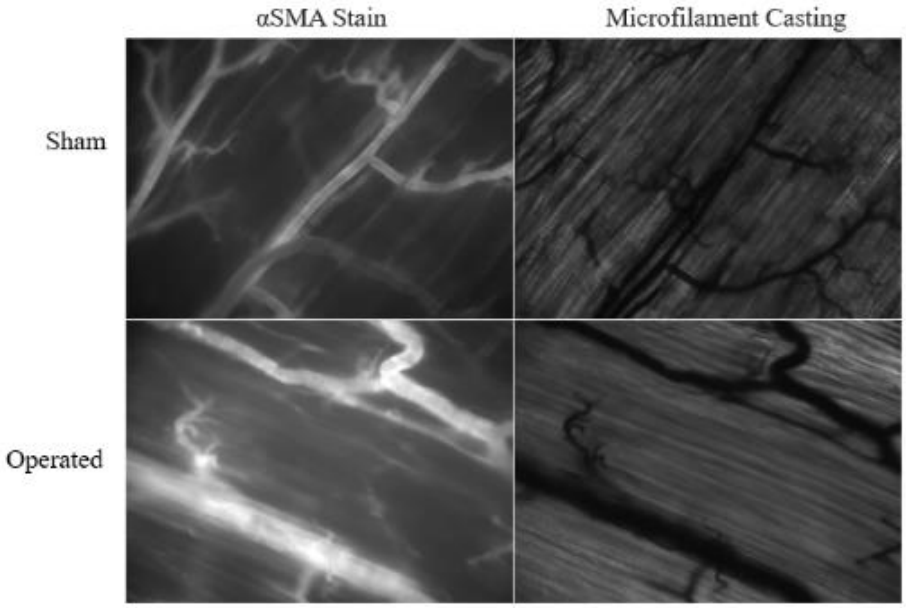

Replicate N1: Lean, Vehicle

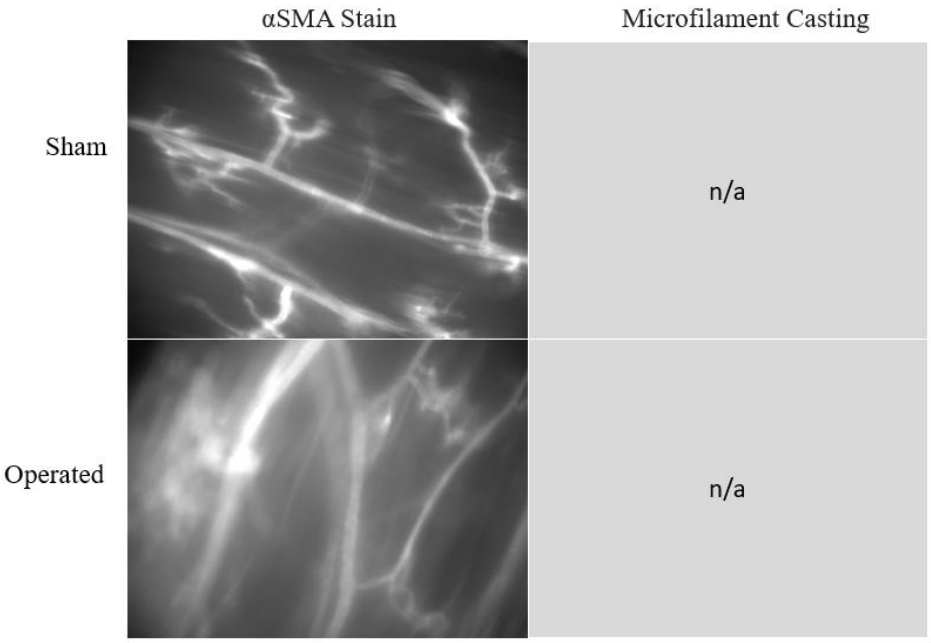

Replicate N1: DIO, Vehicle

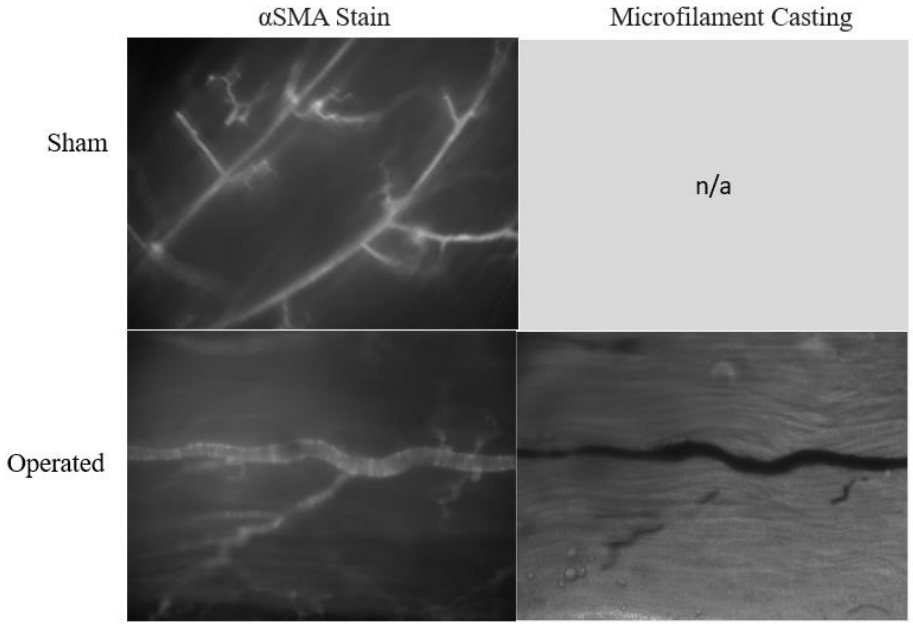

Replicate N2: Lean, Cell

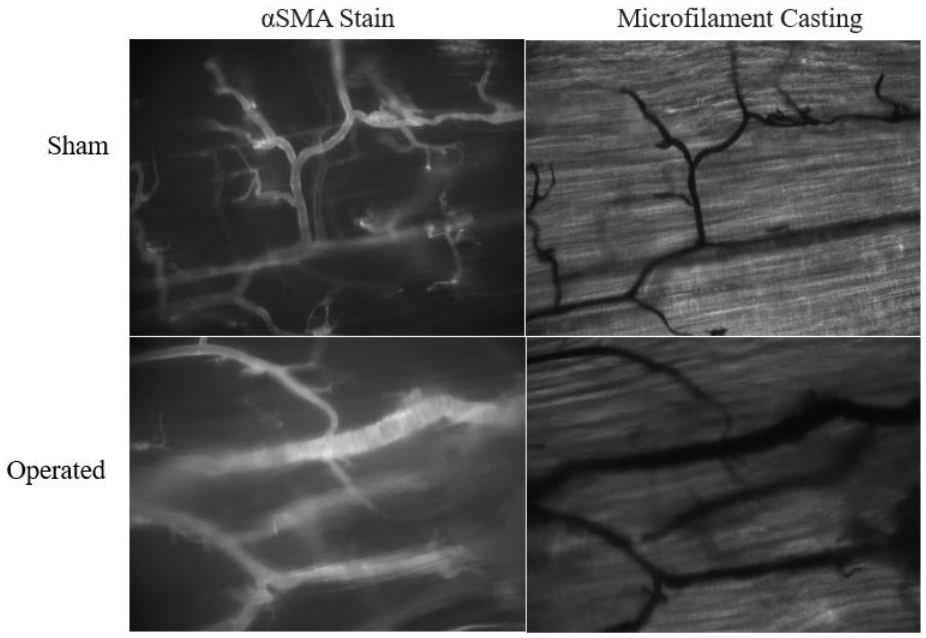

Replicate N2: Lean, Vehicle

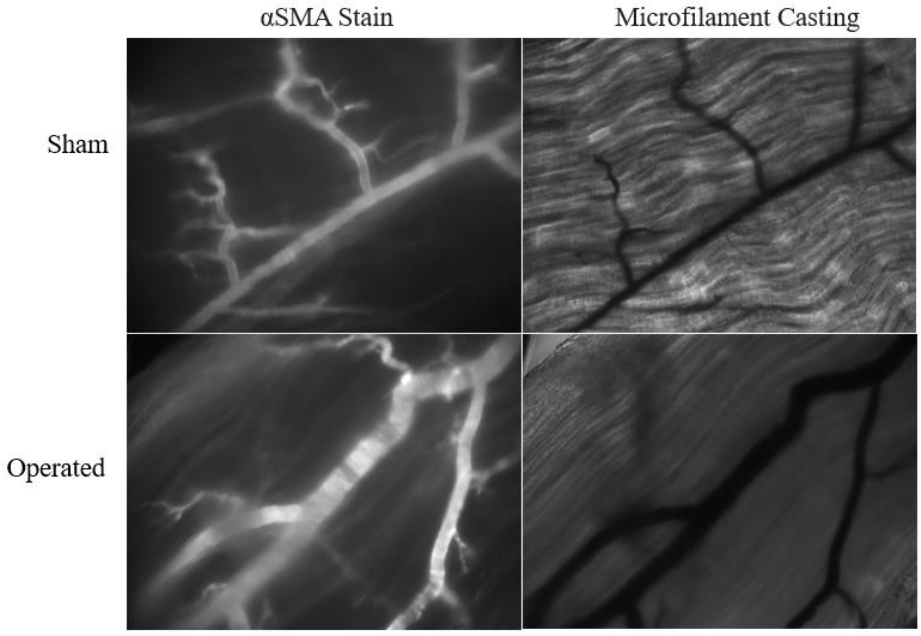

Replicate N2: DIO, Vehicle

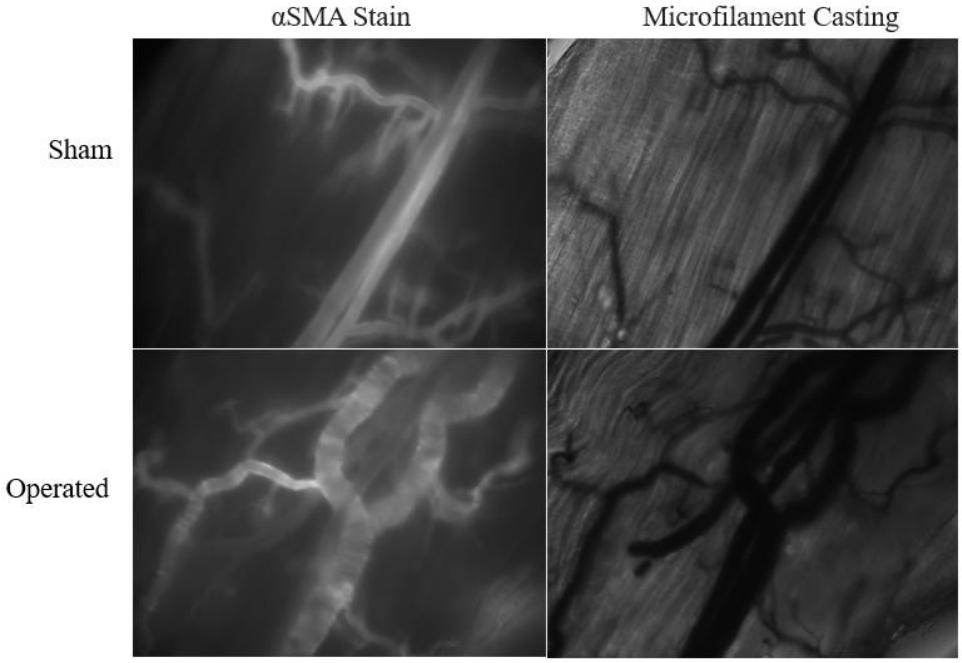

Replicate N3: Lean, Cell

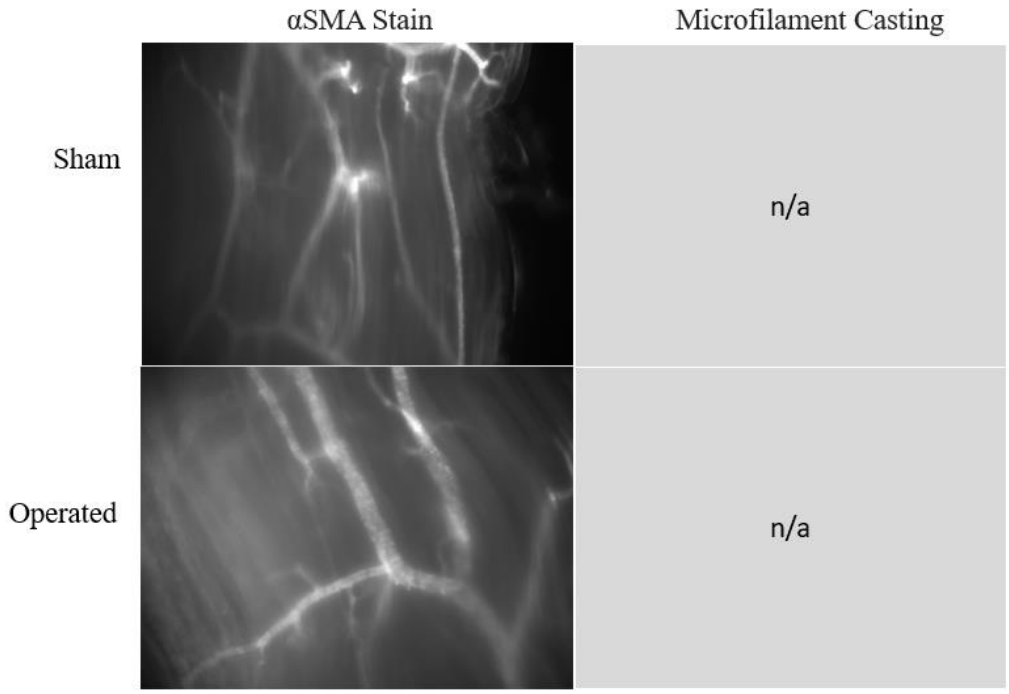

Replicate N3: DIO, Cell

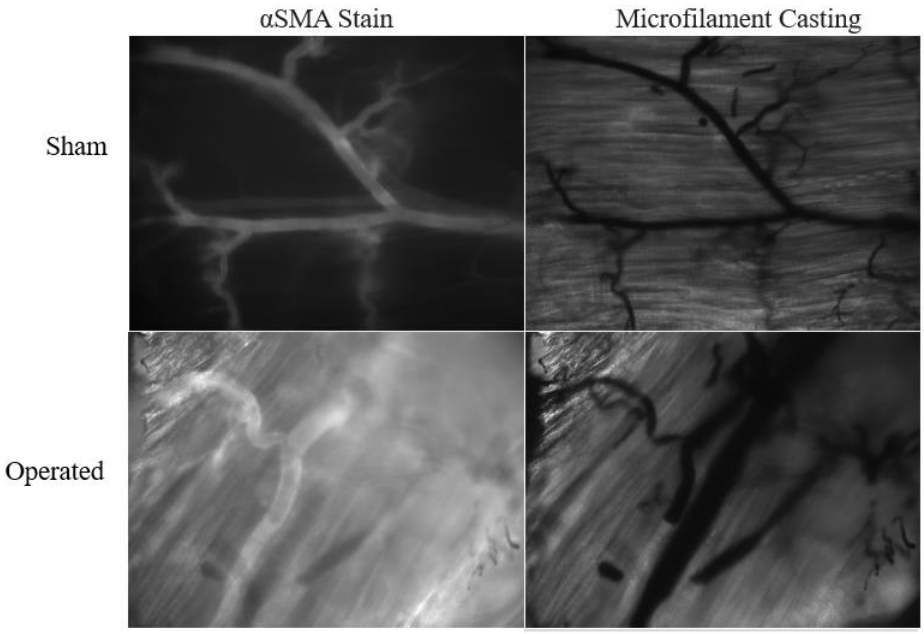

Replicate N3: DIO, Vehicle

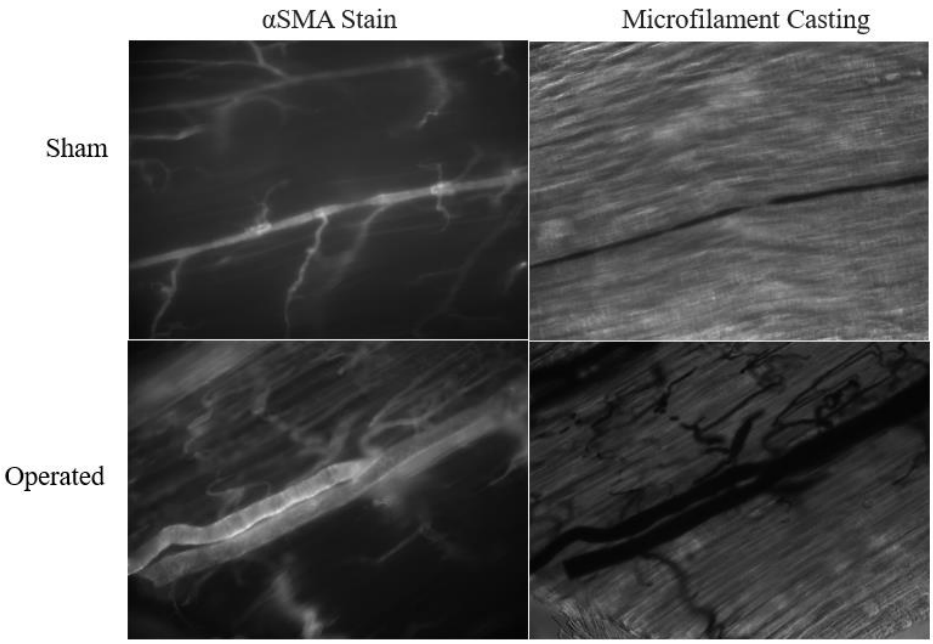

Replicate N4: DIO, Cell

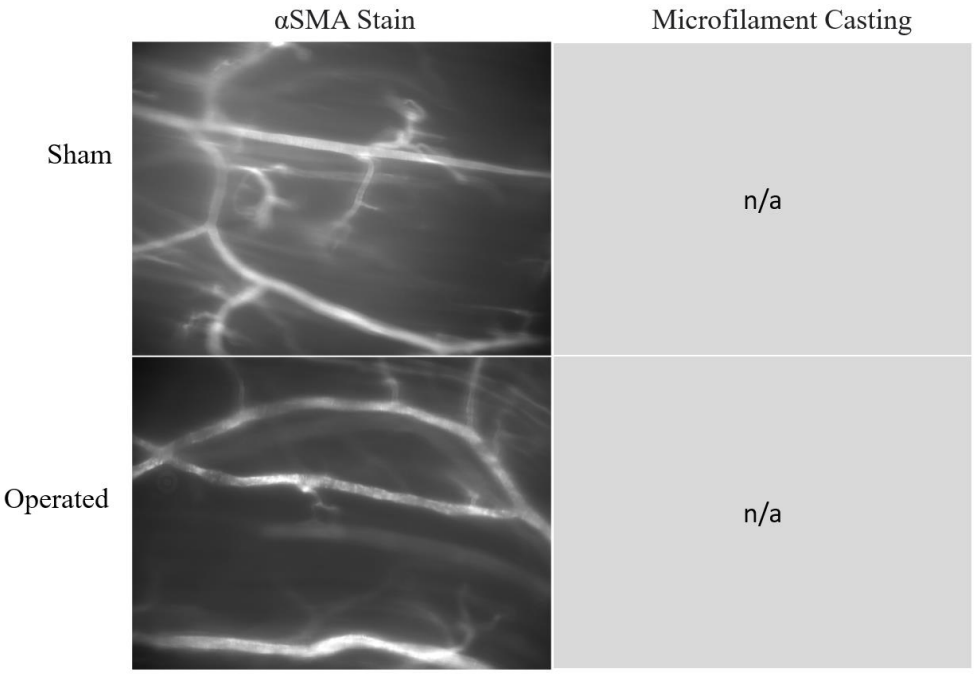

Replicate N4: DIO, Vehicle

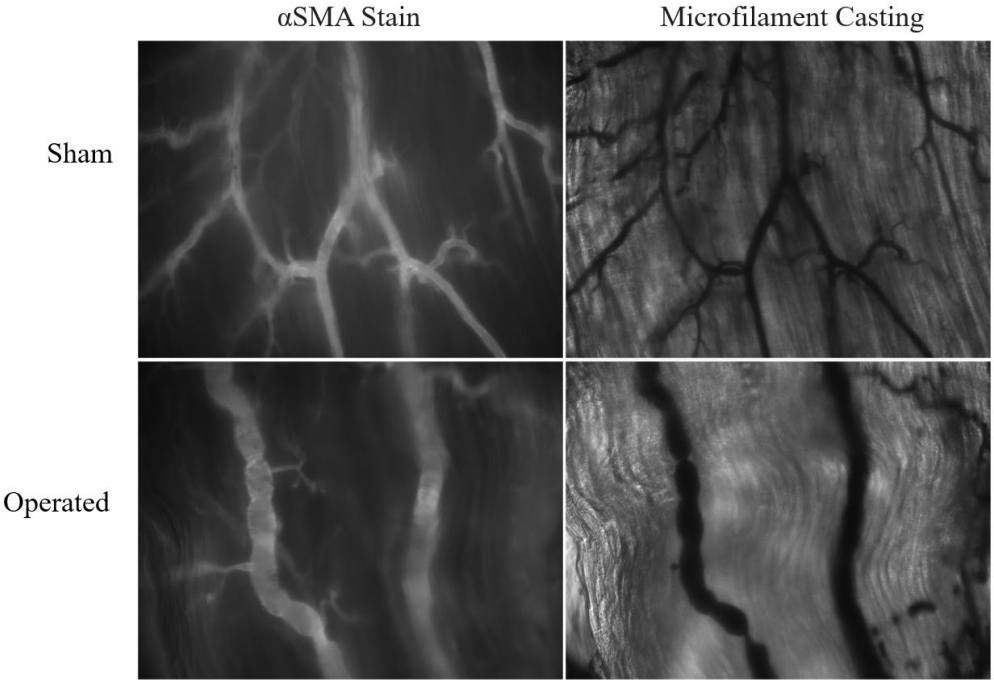

Replicate N5: DIO, Cell

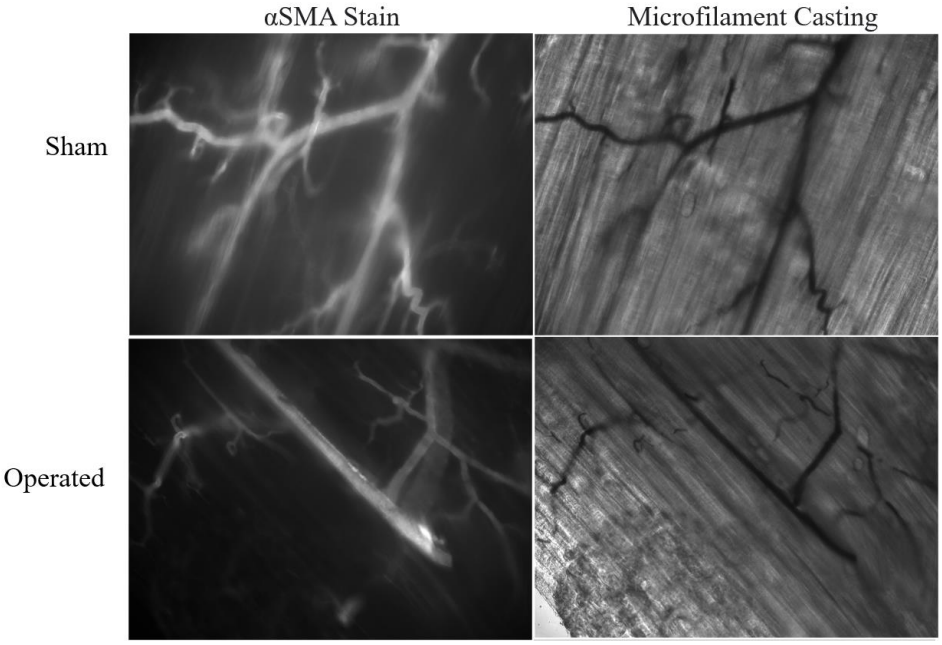

Replicate N5: DIO, Vehicle

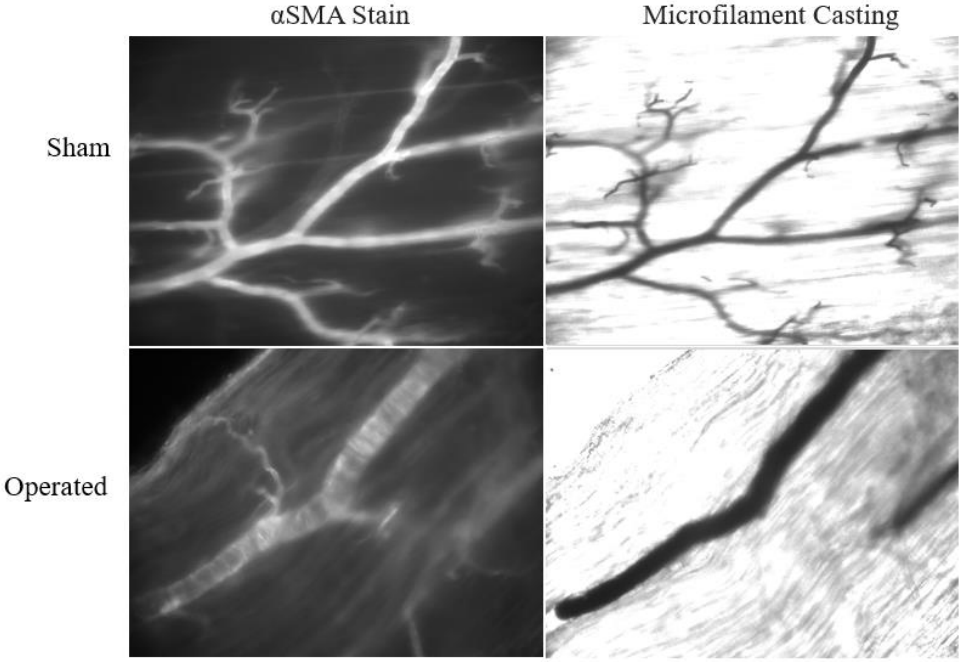

Replicate N6: DIO, Cell

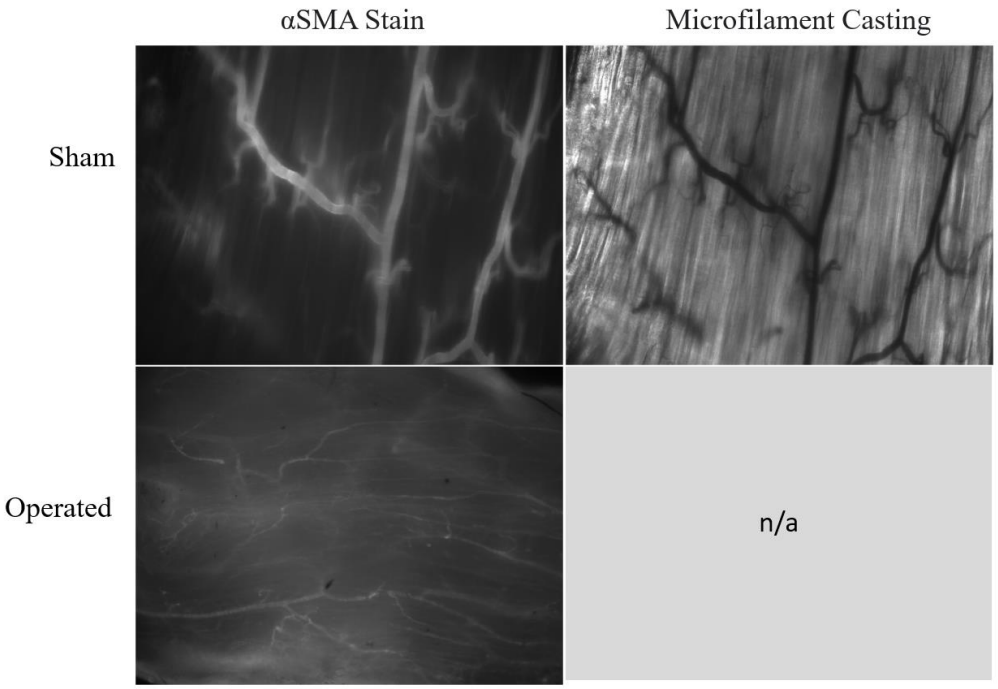

Replicate N6: DIO, Vehicle

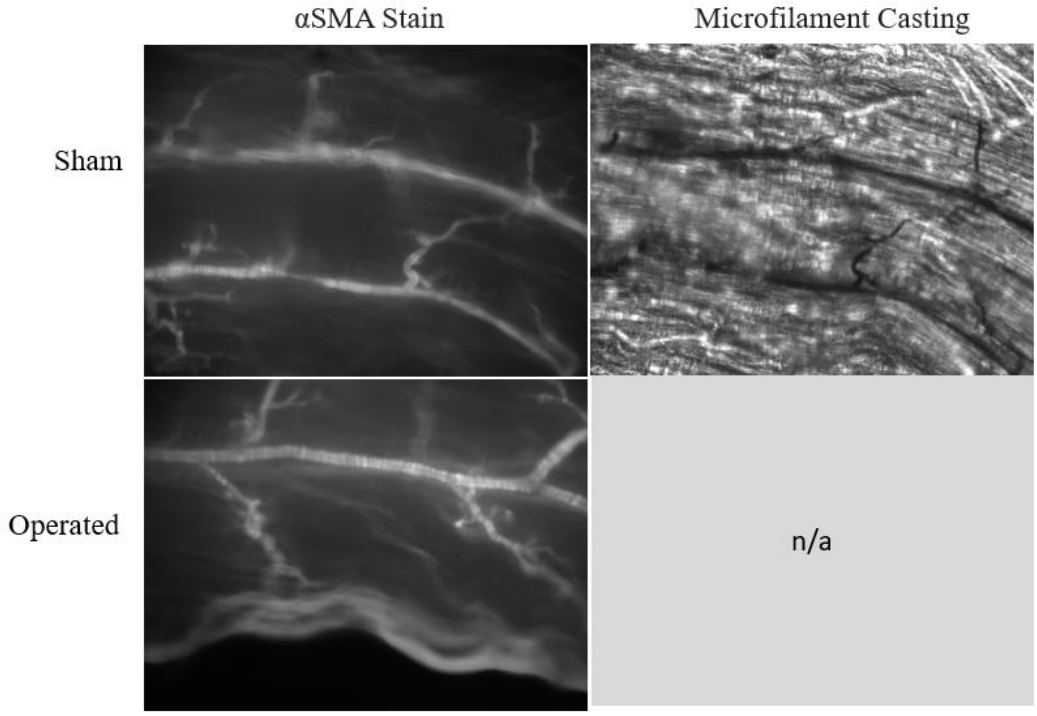

Replicate N7: DIO, Vehicle

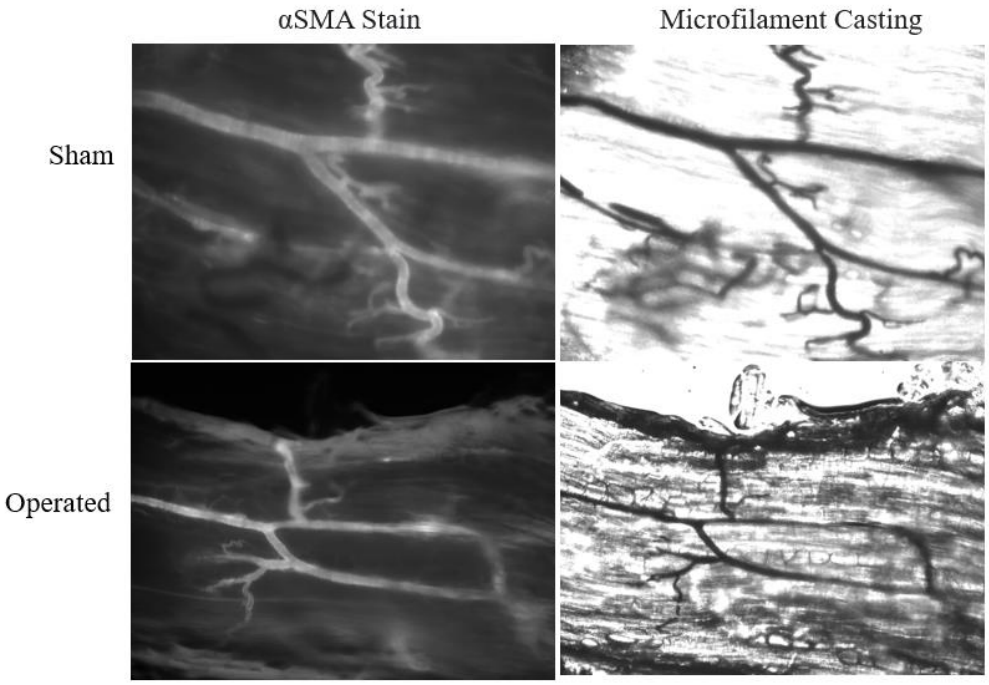

Replicate N7: DIO, Cell

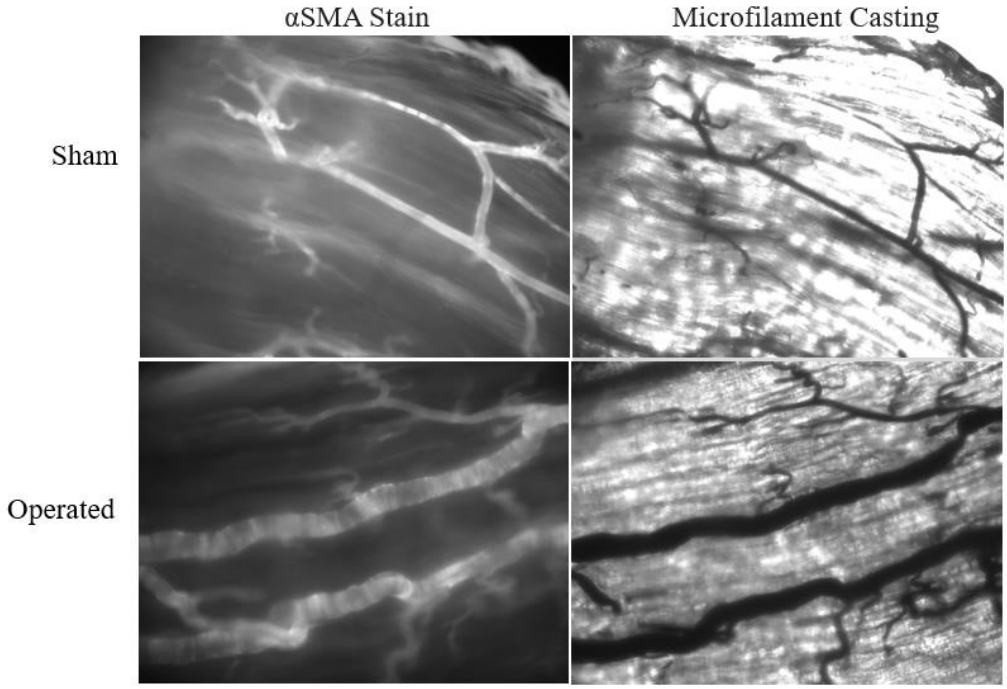

Replicate N8: DIO, Vehicle

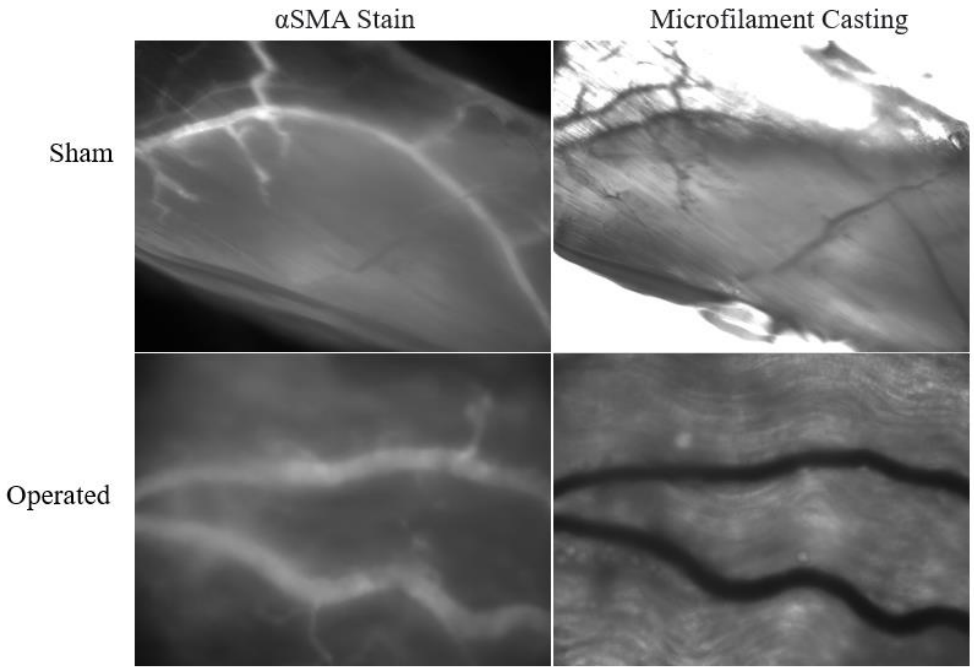

Replicate N8: DIO, Cell

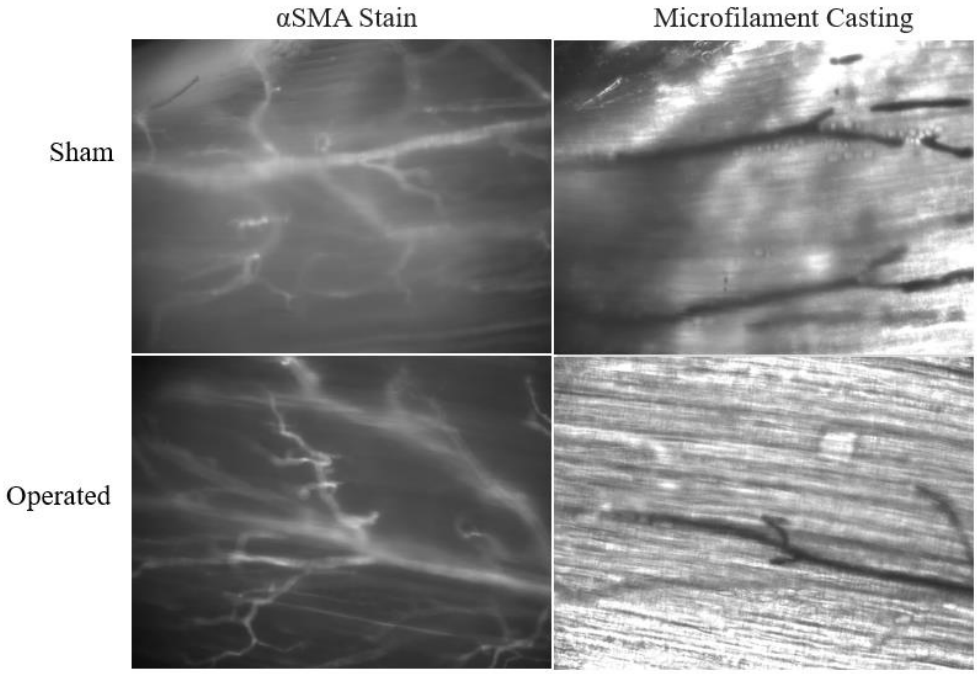

Replicate N9: DIO, Cell

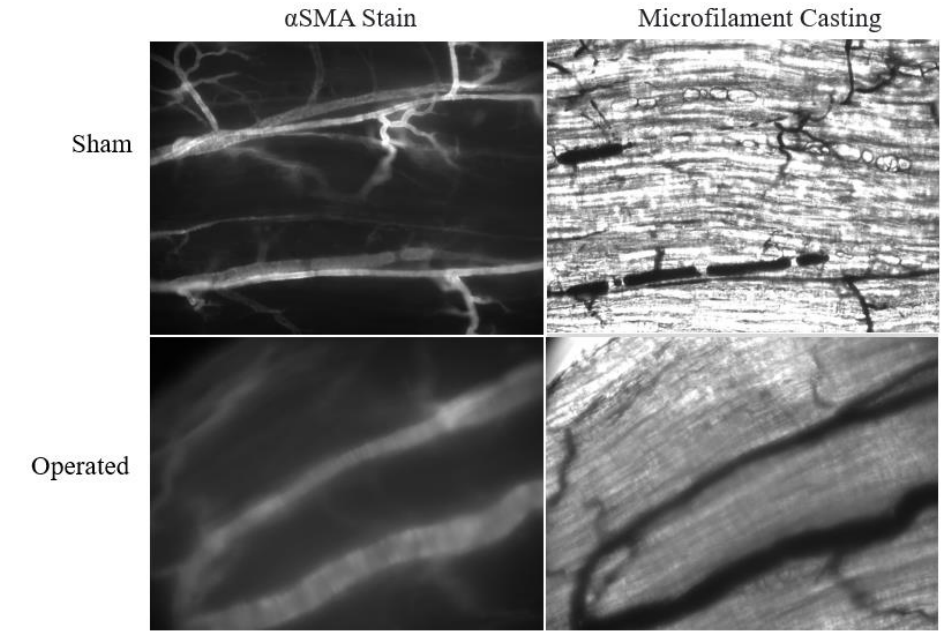

Replicate N10: DIO, Cell

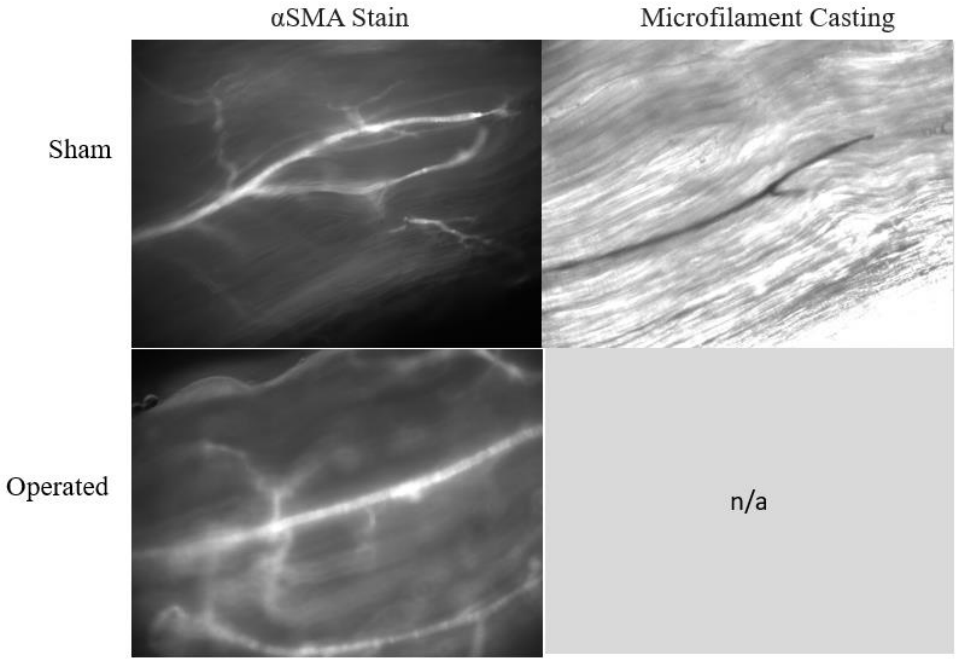

Appendix B: Raw Data

ASMA Immunofluorescence (Outer Diameter) and Vascular Casting (Inner Diameter)

Replicate	Phenotype	Hindlimb	Treatment	Outer Diameter (µm)	Inner Diameter (µm)	Wall Thickness (µm)
1	Lean	Operated	Vehicle	40.94	24.56	16.39
1	DIO	Operated	Vehicle	86.19	71.59	14.60
1	Lean	Operated	Cells	68.00	61.88	6.11
1	DIO	Operated	Cells	68.08	59.21	8.87
1	Lean	Sham	Vehicle	28.32	n/a	n/a
1	DIO	Sham	Vehicle	14.15	n/a	n/a
1	Lean	Sham	Cells	35.02	28.68	6.34
1	DIO	Sham	Cells	38.20	31.36	6.83
2	Lean	Operated	Cells	77.69	68.12	9.57
2	Lean	Operated	Vehicle	89.19	84.44	4.75
2	DIO	Operated	Vehicle	93.24	72.91	20.33
2	Lean	Sham	Cells	33.23	22.28	10.95
2	Lean	Sham	Vehicle	46.76	36.99	9.77
2	DIO	Sham	Vehicle	76.62	66.77	9.85
3	Lean	Operated	Vehicle	100.16	93.03	7.14
3	DIO	Operated	Cells	87.30	63.33	23.97
3	DIO	Operated	Vehicle	84.69	75.94	8.75
3	Lean	Sham	Vehicle	46.53	n/a	n/a
3	DIO	Sham	Cells	55.94	36.65	19.29
3	DIO	Sham	Vehicle	90.42	76.53	13.89
4	DIO	Operated	Cells	33.59	n/a	n/a
4	DIO	Operated	Vehicle	86.28	81.05	5.23
4	DIO	Sham	Cells	33.17	n/a	n/a
4	DIO	Sham	Vehicle	37.04	28.50	8.54
5	DIO	Operated	Cells	69.20	46.85	22.35
5	DIO	Operated	Vehicle	109.49	95.94	13.55
5	DIO	Sham	Cells	49.74	35.83	13.91
5	DIO	Sham	Vehicle	46.98	29.46	17.52
6	DIO	Operated	Cells	19.54	n/a	n/a
6	DIO	Operated	Vehicle	39.32	n/a	n/a
6	DIO	Sham	Cells	45.96	32.38	13.58
6	DIO	Sham	Vehicle	33.42	25.38	8.04
7	DIO	Operated	Vehicle	66.51	52.39	14.12
7	DIO	Operated	Cells	98.42	87.07	11.36
7	DIO	Sham	Vehicle	35.13	27.00	8.13
7	DIO	Sham	Cells	38.42	27.15	11.27
8	DIO	Operated	Vehicle	88.43	69.77	18.66

8	DIO	Operated	Cells	46.85	38.40	8.45
8	DIO	Sham	Vehicle	43.19	25.91	17.28
8	DIO	Sham	Cells	37.19	33.00	4.19
9	DIO	Operated	Cells	125.62	105.35	20.27
9	DIO	Sham	Cells	56.40	43.26	13.14
10	DIO	Operated	Cells	45.28	n/a	n/a
10	DIO	Sham	Cells	34.10	22.57	11.52

Appendix C: Femoral Artery Ligation Protocol

Date_____ **Hindlimb Ischemia Surgery – Femoral Artery Ligation** Initials _____

Purpose: Simulate arterial occlusion

Materials

Pre-sterilize in autoclave

____1. Standard pattern forceps (1)
____2. Fine forceps- S&T (2)
____3. Ultrafine forceps- 545 (1)
____4. Curved iris scissors (1)
____5. Gauze sponges- 2x2" and 4x4"
____6. Cotton swabs
____7. 6.0 silk suture (2 x 1-inch pieces)
____8. 7.0 prolene suture
____9. Needle holder (1)

Obtain in surgery suite

____10. Depilatory cream- Veet
____11. Non-sterile cotton swabs
____12. Non-sterile gauze sponges (2x2 and 4x4)
____13. Chlorhexidene diacetate (Nolyasan)
____14. 1-mL insulin syringes (2)
____15. Buprenorphine analgesic (0.03 mg·ml^{-1})
____16. Ear punch
____17. Veterinary ointment, applied to corneas
____18. Surgical tape
____19. FST heat pad w/ rectal probe
____20. Surgical scrubs
____21. Sterile petri dish (1)
____22. Sterile 5-mL syringe (1)
____23. Sterile saline
____24. Isolation mask and cap
____25. Sterile gloves
____26. Recovery bin and heat pad
____27. 70% isopropyl alcohol (IPA), to disinfect stage and microscope

Animal preparation

____28. Spray surgery area with Nolyasan.
____29. Place animal in induction chamber.
____30. Open oxygen cylinder. Set flow high and isofluorane to 5%.
____31. Once anesthetized, weigh animal and move to preparatory bench in a supine position.
____32. Reduce isoflurane to 1-3% and flow to 0.5-1.5 l·min^{-1}.
____33. Gently apply a generous amount of veterinary ointment to eyes using a cotton swab and let sit for 1-3 minutes
____34. Apply depilatory cream to hindlimb with a cotton swab and let sit for 1-3 minutes.
____35. Spray a 2x2 gauze sponge with Nolyasan and wipe hindlimb clean of cream and hair.
____36. Flip animal over and apply ear punch to the skin, avoid cartilage
____37. Administer pre-op buprenorphine dose (0.075 mg·kg^{-1}) by subcutaneous injection.
____38. Cover heat pad with a 4x4 gauze sponge and transfer animal to surgery stage.
____39. Apply lubricant to rectal probe and insert. Set thermo-controller to 35°C.
____40. Change into surgical scrubs and wash hands/forearms.
____41. Open sterile instrument tray and sterile pack.
____42. Obtain sterile petri dish in sterile field and fill with sterile saline, using a 5-mL syringe.
____43. Put on mask, cap, and position/focus microscope before putting on sterile gloves.

Surgery

____44. Make a small incision on the middle, medial aspect of the hindlimb, directly over the neurovascular bundle.
____45. Extend incision to the abdominal wall, reaching the fat pad
____46. Blunt dissect subcutaneous connective tissue to maximize surgical exposure.
____47. Blunt dissect and retract epigastric fat pad to expose ligation site, proximal to the popliteal artery and distal to the epigastric.
____48. Blunt dissect connective tissue over bundle and separate nerve from the artery-vein pair.
____49. Use ultrafine forceps to separate the artery from the vein.
____50. Tie off the femoral artery with silk suture.
____51. Blunt dissect a pocket underneath the gracilis muscle. Retrieve the bio-printed construct from the incubator and implant the construct in the pocket.
____52. Use 7-0 prolene suture to close the incision. Begin with a surgeons square knot, continue with spiral suturing, and finish with an instrument square knot.
____53. Repeat steps 44-48 on the sham side, contralateral without artery/vein/nerve separation
____54. Repeat step 52 on the sham side

Post-Surgical

____55. Administer post-op buprenorphine dose (0.075 mg·kg^{-1}) by subcutaneous injection.
____56. Microwave recovery heat pad for ~1-2 min.
____57. Transfer animal to recovery previously disinfected bin). Leave animal there until ambulatory
____58. Turn off isoflurane, flow, and close oxygen.
____59. Wipe down surgical area with IPA and wash all instruments.

Appendix D: Perfusion Fixation Protocol

Date_____ **Perfusion Fixation** Initials_____

Mouse Information
DOB:_____
Sex: _____
Tag: _____
Genotype/strain: _____
Cage:_____
Weight(g): _____

Materials
Non-Sterilize Dissection Instruments
____1. Forceps (1)
____2. Fine forceps (2)
____3. Bone scissors (1)
____4. Curved Iris scissors (1)
____5. Microdissection scissors (1)
____6. Vascular clamp (1)
____7. Castroviejos

Obtained in surgery suite
____8. Tape
____9. 20 mL syringes (2)
____10. 5 mL syringe (1)
____11. Syringe pump
____12. Petri-dish
____13. Bench cover
____14. Depilatory cream
____15. Clippers
____16. Veterinary ointment
____17. Heating pad
____18. Catheter
____19. Non-sterile saline
____20. Cotton swabs
____21. Gauze sponges
____22. Saran wrap

Vasodilator Cocktail Preparation
____23. Turn on water bath to 37ºC
____24. 400 µL heparin
____25. 1mL SNP(orange)
____26. 600µL Adenosine(clear)
____27. 38mL PBS solution
____28. 5 mL 4% Paraformaldehyde (PFA)
____29. Thaw SNP, Adenosine and PFA
____30. Add heparin, SNP, Adenosine, and PBS solution together in a 50mL conical
____31. Place vasodilator cocktail in water bath

Procedure Preparation
____32. Obtain saline filled petri-dish, cotton swab, and instruments

Fixation
____33. Remove hair on both legs by shaving & depilation
____34. Tape animal in supine position to 4X4 gauze sponge over heating pad
____35. Expose muscles of interest and blunt dissect to aid in removal post-fixation, then cover with saran wrap
____36. Fill 20mL syringe with 20 mL warm Vaso D, load into syringe pump and attach catheter
____37. Flow liquid through the catheter to the tip to prevent air from being injected into circulatory system
____38. Lift skin from muscle in abdominal region and cut a window over the sternum
____39. Lift sternum and cut connective tissue under
____40. Use bone scissors in hole to quickly cut through the ribs to the armpit on both sides
____41. Clamp sternum with castroviejos and reflect towards mouse's head
____42. Cut diaphragm with curved iris scissors to open chest cavity
____43. Cut away excess tissue around the heart
____44. Make a small incision in the apex of the heart
____45. Insert catheter and clamp with vascular clamp and cut right atrium
____46. Inject Vaso D solution into animal approximately 20mL X 2 (5mL/min), soaking up excess blood and fluids with gauze sponges
____47. Inject 5 mL PFA (4 mL/min)
____48. Dissect out muscles of interest using fine forceps and microdissection scissors
____49. Turn off water bath, cover scope, turn off oxygen, turn off isofluorane, and clean instruments

Notes
_____
_____
_____
_____
_____
_____

Appendix E: Vascular Casting Protocol

Microfil casting and dissection protocol

Date _____ Microfil Initials _____

Mouse Information

DOB: _____
Sex: _____
Tag: _____
Genotype/strain: _____
Cage: _____
Weight (g): _____

Materials

Non-Sterilize Dissection Instruments

____1. Forceps (1)
____2. Bone Scissors(1)
____3. Skin Scissors (1)
____4. Hemostats(1)
____5. Spring Scissors for Ventricle (1)
____6. Vascular clamp (1)

Obtained in surgery suite

____7. Tape
____8. 20mL Syringe (1)
____9. Bench cover
____10. Heating pad
____11. Catheter/Stopcock/Blunt needle (PE-100)
____12. Isoflurane Anesthetic
____13. Gauze squares

Vasodilator Cocktail Preparation

____14. Turn on water bath to 37℃
____15. 400 µL heparin
____16. 1mL SNP (orange)
____17. 600µL Adenosine (clear)
____18. 38mL PBS solution
____19. Thaw SNP and Adenosine
____20. Add heparin, SNP, Adenosine, and PBS solution together in a 50mL conical
____21. Place vasodilator cocktail in water bath

Microfil Cocktail Preparation

____22. 2mL Microfil MV-122
____23. 1.25mL Microfil HV-Diluent
____24. 1.25mL Microfil MV-Diluent
____25. Add MV-122, HV-Diluent & MV-Diluent into a 14mL conical, vortex, place in bath

Procedure Preparation

____26. Weigh animal
____27. Obtain saline filled petri-dish, cotton swab, and instruments

Fixation

____28. Anesthize mouse with Isoflurane
____29. Heat up heat pad in microwave and wrap with bench cover when warm
____30. Remove hindlimb hair on both legs by shaving
____31. Tape animal down to heated bench cover
____32. Separate skin from muscle from the abdomen to the top of the thoracic cavity
____33. Fill 20mL syringe with warm Vaso D
____34. Cut through abdomen close to diaphragm
____35. Quickly cut through the ribs and diaphragm to open chest cavity and clamp back with hemostats
____36. Cut away excess tissue around the heart
____37. Make a small incision in the apex of the heart
____38. Insert catheter and clamp with vascular clamp and cut right atria
____39. Inject Vaso D solution into animal approximately 20mL at 5mL/min x2
____40. Add .2mL of curing agent to Microfil
____41. Inject 1mL of Microfil Cocktail (.5mL/min)
____42. Pause microfilm and ligate both ankles with silk suture once Microfil has passed the knee. Resume Microfil.
____43. Repeat step 41 until satisfied with fill.
____44. Remove mouse from heat pad and take out catheter (keep heart clamped)
____45. Place mouse in bag (cover open wounds with saran wrap) and let sit overnight at room temp
____46. Cover scope, turn off water bath, turn off oxygen, turn off Isoflurane, clean instruments

Dissection Date: _____

Non-Sterilized Dissection Instruments

____47. Fine Forceps (2)
____48. Forceps (1)
____49. Iris Scissors (1)
____50. Dissection scissors (1)

Obtained in surgery suite

____51. Non-sterile saline
____52. Cotton swab
____53. Bench cover
____54. Tape
____55. Petri Dishes (2)
____56. Cover Slips (2)
____57. Disposable pipettes (1)
____58. 25% ethanol
____59. Dissect chosen muscles and place on cover slip and then in labeled petri dish of 25% ethanol
____60. Cover scope and clean instruments

Notes:

_____
_____
_____
_____
_____
_____

Appendix F: ASMA Staining and Imaging Protocol

Materials

24-well culture plates (Cat#: 3738, Corning Incorporated)
PBS
0.1% Saponin (Cat#: 47036, Sigma-Aldrich)
2% Bovine Serum Albumin (Cat# B6917, Sigma Aldrich)
Monoclonal Anti-Alpha Smooth Muscle Actin, Cy3 Conjugate (Cat#: C6198, Sigma-Aldrich)
Slides
Coverslips
Parafilm
Aluminum foil

Staining

1. Using forceps, remove muscle from PBS (stored in microcentrifuge tube at 4°C) and place in a single well of a 24-well culture plate.
2. Prepare antibody solution containing 1:200 1A4 clone (alpha-smooth muscle actin, Cy3 conjugate) in 0.1% saponin (reconstituted in PBS), 2% BSA (reconstituted in PBS) in PBS, using 0.3mL of solution per muscle.
3. Incubate muscle in antibody solution for 3 nights (72 hours) at 4°C). **(Note: Critical step—3 nights crucial for bright staining) by gently pipetting solution over muscle.)**
4. Wash in 0.1% saponin in PBS 3x for 20 minutes at room temperature. Cover plate with foil during each wash.
5. Wash in plain PBS for 30 minutes. Cover with foil during each wash.
6. Place 1-2 drops of 50/50 PBS and Glycerol onto slide.
7. Remove muscle from well using forceps and place on a slide.
8. Add 1-2 drops of 50/50 PBS and Glycerol to the top of the muscle and place cover slips over the muscle.
9. Paint edges of coverslip with clear nail polish to create a seal and prevent tissue desiccation.
10. Store slides at 4°C wrapped in foil or an opaque container between imaging.

Imaging

11. Image using a standard fluorescent microscope. (Cy3 excitation: 550 nm, emission: 570 nm)

Appendix G: Statistical Analysis

Comparisons between Outer Diameter of Operated and Sham Hindlimbs

Analysis: Tukey Pairwise and 2-sample T-test

Tukey Pairwise Comparisons: Hindlimb

Grouping Information Using the Tukey Method and 95% Confidence

Hindlimb	N	Mean	Grouping
Operated	22	73.8183	A
Sham	22	43.4508	B

Means that do not share a letter are significantly different.

WORKSHEET 6

Two-Sample T-Test and CI: Outer Diameter (µm), Hindlimb

Method

μ_1: population mean of Outer Diameter (µm) when Hindlimb = Operated
μ_2: population mean of Outer Diameter (µm) when Hindlimb = Sham
Difference: $\mu_1 - \mu_2$

Equal variances are not assumed for this analysis.

Descriptive Statistics: Outer Diameter (µm)

Hindlimb	N	Mean	StDev	SE Mean
Operated	22	73.8	26.9	5.7
Sham	22	43.5	16.1	3.4

Estimation for Difference

Difference	95% CI for Difference
30.37	(16.77, 43.97)

Test

Null hypothesis $H_0: \mu_1 - \mu_2 = 0$
Alternative hypothesis $H_1: \mu_1 - \mu_2 \neq 0$

T-Value	DF	P-Value
4.54	34	0.000

Comparisons between Outer Diameter of Phenotype (DIO v. Lean) and Treatment (Cells v. Vehicle)

Analysis: 2-way ANOVA and Tukey Pairwise

WORKSHEET 6

General Linear Model: Outer Diameter (μm) versus Phenotype, Treatment

Method

Factor coding (-1, 0, +1)

Factor Information

Factor	Type	Levels	Values
Phenotype	Fixed	2	DIO, Lean
Treatment	Fixed	2	Cells, Vehicle

Analysis of Variance

Source	DF	Adj SS	Adj MS	F-Value	P-Value
Phenotype	1	89.6	89.58	0.12	0.731
Treatment	1	420.7	420.66	0.56	0.458
Phenotype*Treatment	1	40.7	40.74	0.05	0.817
Error	40	29898.3	747.46		
Total	43	30835.7			

Model Summary

S	R-sq	R-sq(adj)	R-sq(pred)
27.3397	3.04%	0.00%	0.00%

Coefficients

Term	Coef	SE Coef	T-Value	P-Value	VIF
Constant	57.80	5.00	11.56	0.000	
Phenotype					
DIO	1.73	5.00	0.35	0.731	1.03
Treatment					
Cells	-3.75	5.00	-0.75	0.458	1.47
Phenotype*Treatment					
DIO Cells	-1.17	5.00	-0.23	0.817	1.46

Regression Equation

Outer Diameter (μm) = 57.80 + 1.73 Phenotype_DIO - 1.73 Phenotype_Lean
- 3.75 Treatment_Cells + 3.75 Treatment_Vehicle
- 1.17 Phenotype*Treatment_DIO Cells + 1.17 Phenotype*Treatment_DIO
Vehicle + 1.17 Phenotype*Treatment_Lean Cells
- 1.17 Phenotype*Treatment_Lean Vehicle

Fits and Diagnostics for Unusual Observations

Obs	Outer Diameter (μm)	Fit	Resid	Std Resid	
8	125.6	54.6	71.0	2.67	R

R Large residual

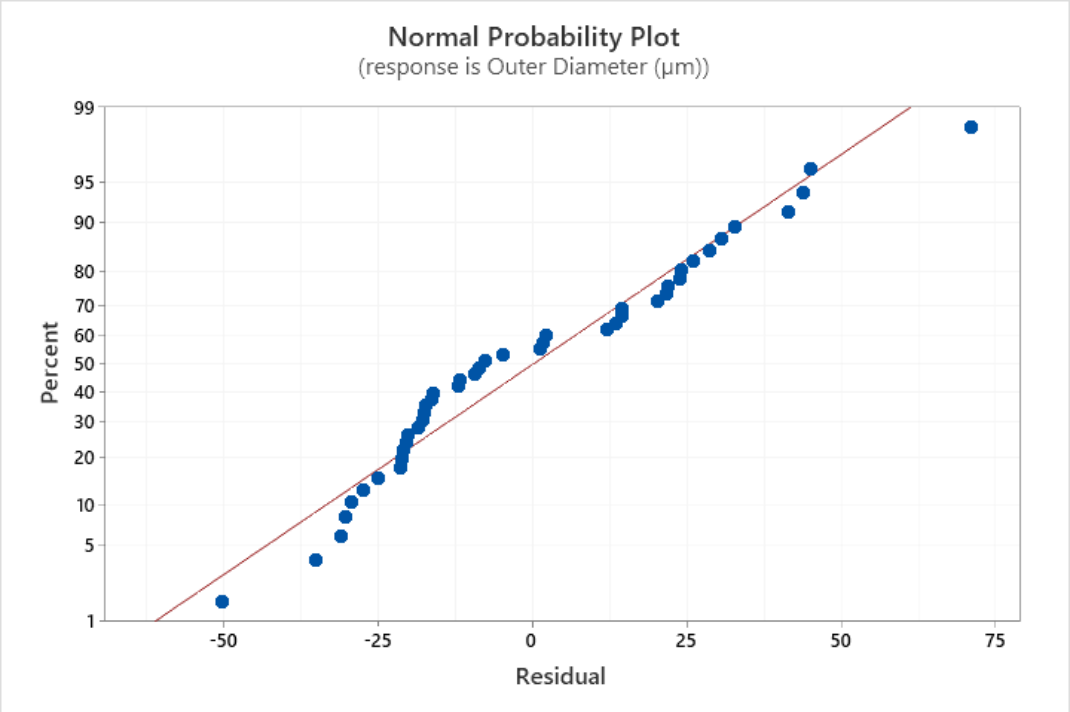
Normal Probability Plot
(response is Outer Diameter (µm))
Percent
99
95
90
80
70
60
50
40
30
20
10
5
1
-50
-25
0
25
50
75
Residual

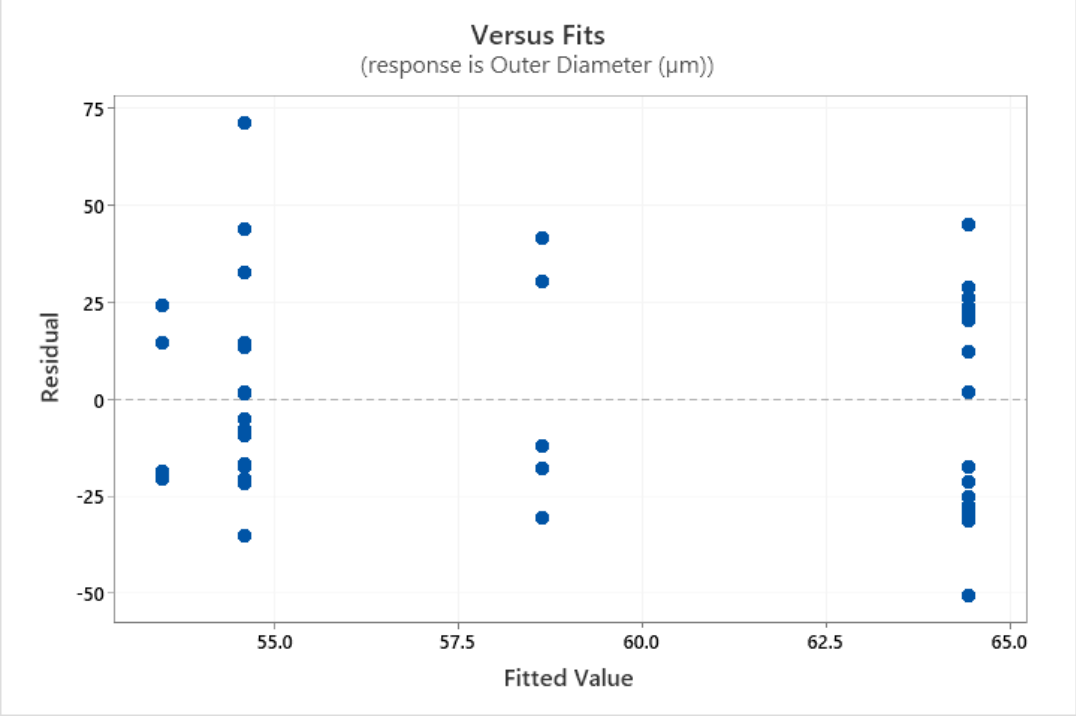
Versus Fits
(response is Outer Diameter (µm))
Residual
75
50
25
0
-25
-50
55.0
57.5
60.0
62.5
65.0
Fitted Value

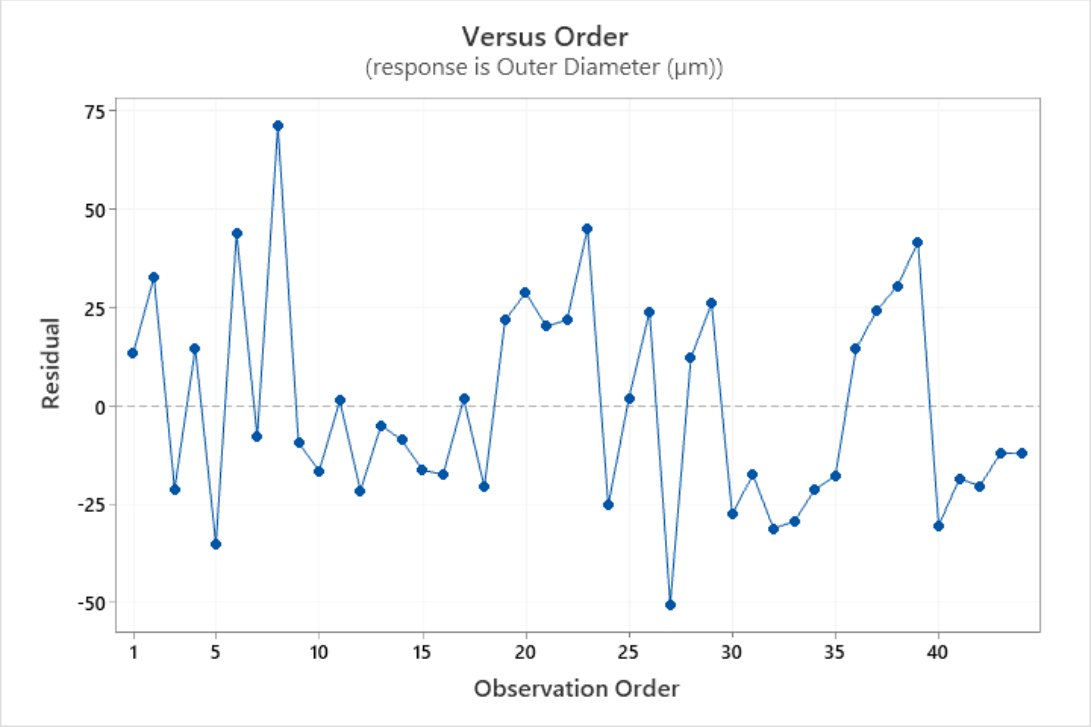
Versus Order
(response is Outer Diameter (µm))
Residual
75
50
25
0
-25
-50
1
5
10
15
20
25
30
35
40
Observation Order

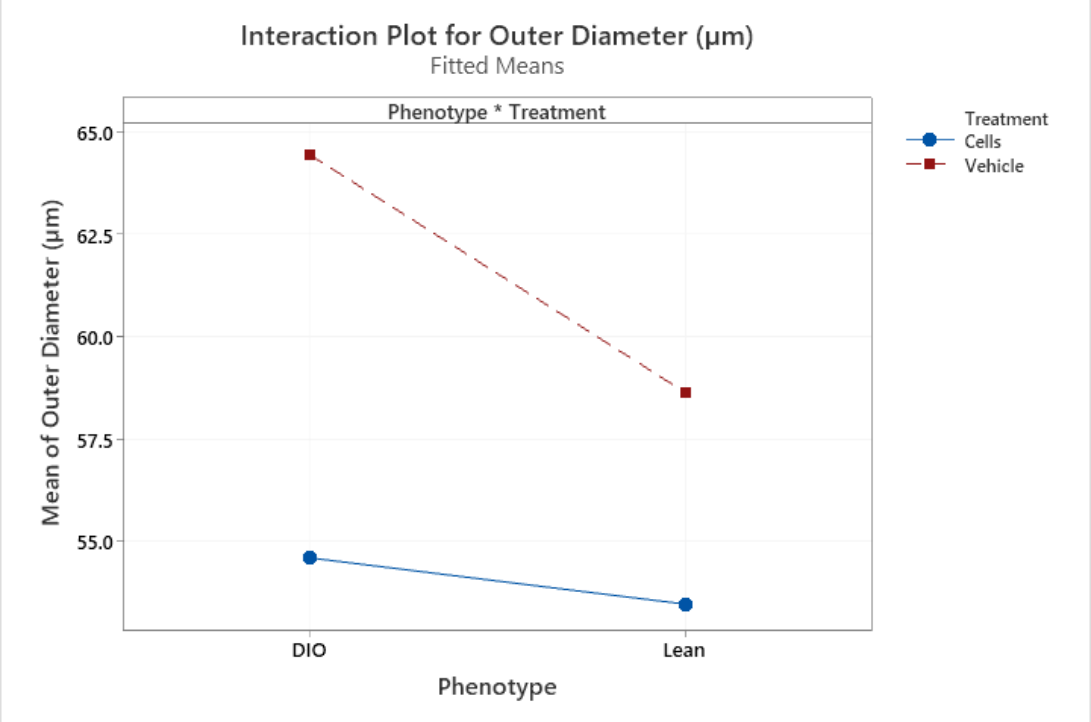
Interaction Plot for Outer Diameter (µm)
Fitted Means
Phenotype * Treatment
Mean of Outer Diameter (µm)
65.0
62.5
60.0
57.5
55.0
DIO
Lean
Phenotype
Treatment
Cells
Vehicle

Grouping Information Using the Tukey Method and 95% Confidence

Phenotype*Treatment	N	Mean	Grouping
DIO Vehicle	16	64.4434	A
Lean Vehicle	6	58.6493	A
DIO Cells	18	54.6108	A
Lean Cells	4	53.4840	A

Means that do not share a letter are significantly different.

('n' refers to number of hindlimbs, not subjects)

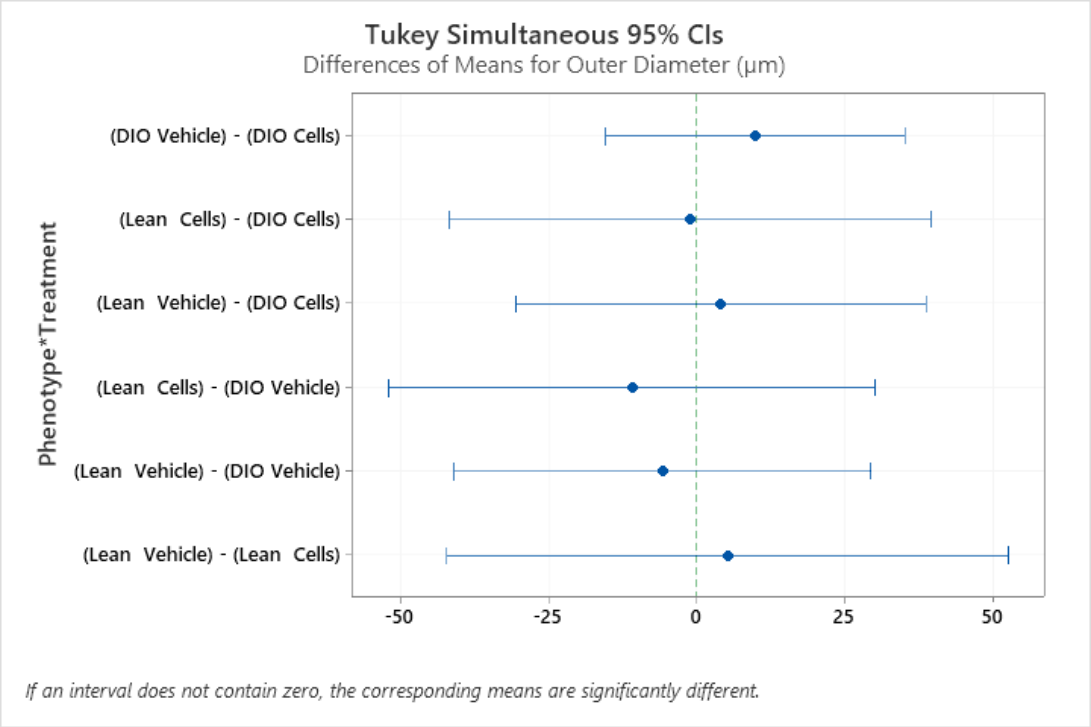

Comparisons between Inner Diameter of Operated and Sham Hindlimbs

Analysis: Tukey Pairwise and 2-sample T-test

ID

Two-Sample T-Test and CI: Inner Diameter (µm), Hindlimb

Method

μ_1: population mean of Inner Diameter (µm) when Hindlimb = Operated
μ_2: population mean of Inner Diameter (µm) when Hindlimb = Sham
Difference: $\mu_1 - \mu_2$

Equal variances are not assumed for this analysis.

Descriptive Statistics: Inner Diameter (µm)

Hindlimb	N	Mean	StDev	SE Mean
Operated	18	69.5	20.7	4.9
Sham	18	35.0	14.5	3.4

Estimation for Difference

Difference	95% CI for Difference
34.56	(22.42, 46.71)

Test

Null hypothesis $H_0: \mu_1 - \mu_2 = 0$
Alternative hypothesis $H_1: \mu_1 - \mu_2 \neq 0$

T-Value	DF	P-Value
5.81	30	0.000

Tukey Pairwise Comparisons: Hindlimb

Grouping Information Using the Tukey Method and 95% Confidence

Hindlimb	N	Mean	Grouping
Operated	18	69.5447	A
Sham	18	34.9834	B

Means that do not share a letter are significantly different.

Comparisons between Inner Diameter of Phenotype (DIO v. Lean) and Treatment (Cells v. Vehicle)

Analysis: 2-way ANOVA and Tukey Pairwise

ID

General Linear Model: Inner Diameter (µm) versus Phenotype, Treat

Method

Factor coding (-1, 0, +1)

Factor Information

Factor	Type	Levels	Values
Phenotype	Fixed	2	DIO, Lean
Treatment	Fixed	2	Cells, Vehicle

Analysis of Variance

Source	DF	Adj SS	Adj MS	F-Value	P-Value
Phenotype	1	0.6	0.554	0.00	0.977
Treatment	1	917.1	917.051	1.43	0.240
Phenotype*Treatment	1	35.1	35.056	0.05	0.816
Error	32	20481.3	640.042		
Total	35	21570.9			

Model Summary

S	R-sq	R-sq(adj)	R-sq(pred)
25.2990	5.05%	0.00%	0.00%

Coefficients

Term	Coef	SE Coef	T-Value	P-Value	VIF
Constant	52.35	5.07	10.32	0.000	
Phenotype					
DIO	-0.15	5.07	-0.03	0.977	1.00
Treatment					
Cells	-6.07	5.07	-1.20	0.240	1.45
Phenotype*Treatment					
DIO Cells	1.19	5.07	0.23	0.816	1.45

Regression Equation

Inner Diameter (µm) = 52.35 - 0.15 Phenotype_DIO + 0.15 Phenotype_Lean
- 6.07 Treatment_Cells + 6.07 Treatment_Vehicle
+ 1.19 Phenotype*Treatment_DIO Cells - 1.19 Phenotype*Treatment_DIO
Vehicle - 1.19 Phenotype*Treatment_Lean Cells
+ 1.19 Phenotype*Treatment_Lean Vehicle

Fits and Diagnostics for Unusual Observations

Obs	Inner Diameter (µm)	Fit	Resid	Std Resid	
6	105.35	47.31	58.03	2.38	R

R Large residual

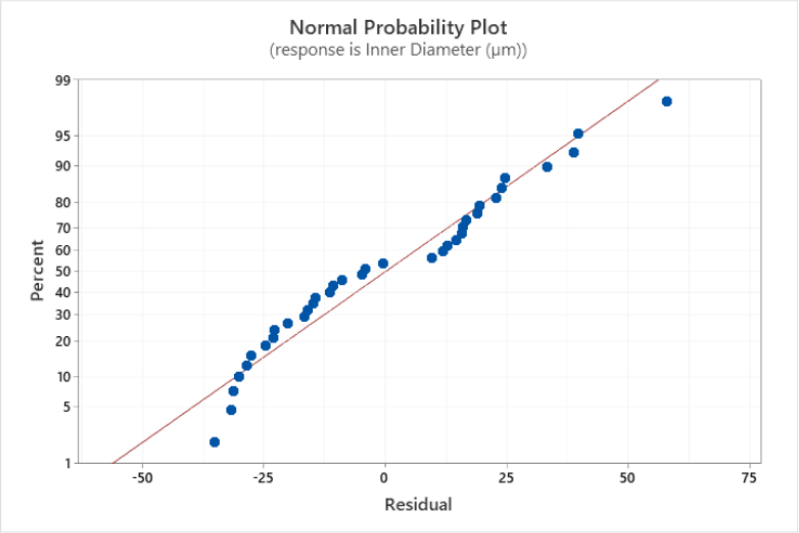
Normal Probability Plot
(response is Inner Diameter (µm))
Percent
99
95
90
80
70
60
50
40
30
20
10
5
1
-50
-25
0
25
50
75
Residual

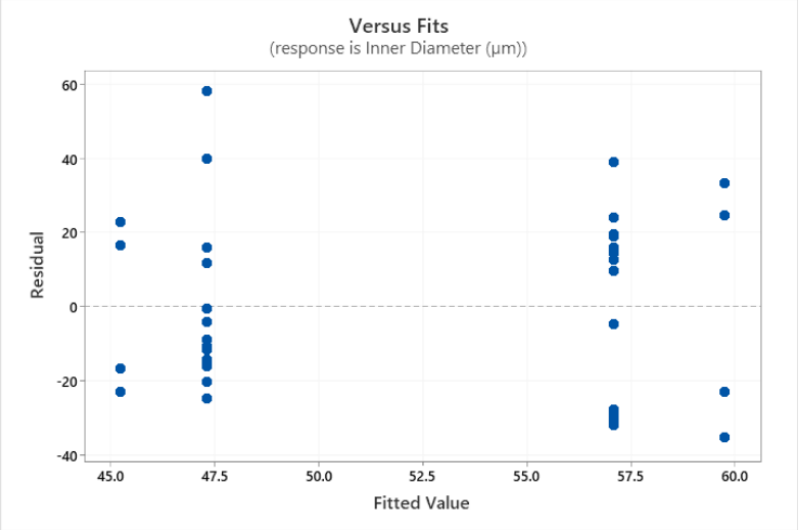
Versus Fits
(response is Inner Diameter (µm))
Residual
60
40
20
0
-20
-40
45.0
47.5
50.0
52.5
55.0
57.5
60.0
Fitted Value

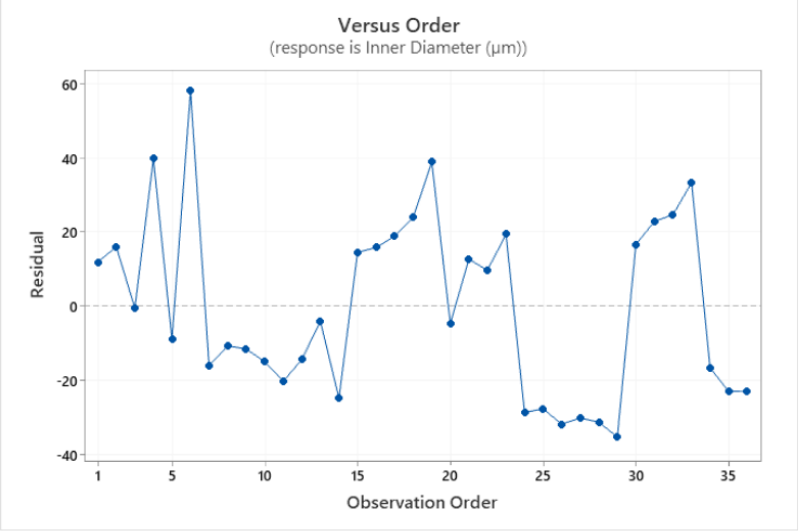
Versus Order
(response is Inner Diameter (µm))
Residual
60
40
20
0
-20
-40
1
5
10
15
20
25
30
35
Observation Order

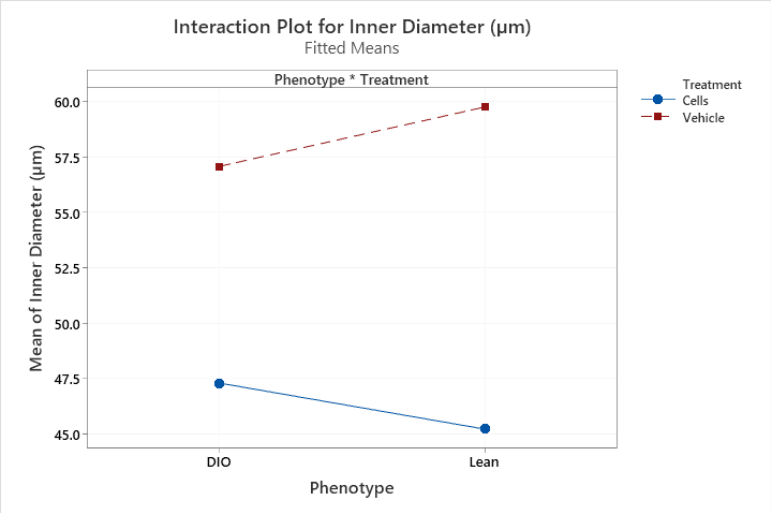

Tukey Pairwise Comparisons: Phenotype*Treatment

Grouping Information Using the Tukey Method and 95% Confidence

Phenotype*Treatment	N	Mean	Grouping
Lean Vehicle	4	59.7531	A
DIO Vehicle	14	57.0810	A
DIO Cells	14	47.3145	A
Lean Cells	4	45.2393	A

Means that do not share a letter are significantly different.

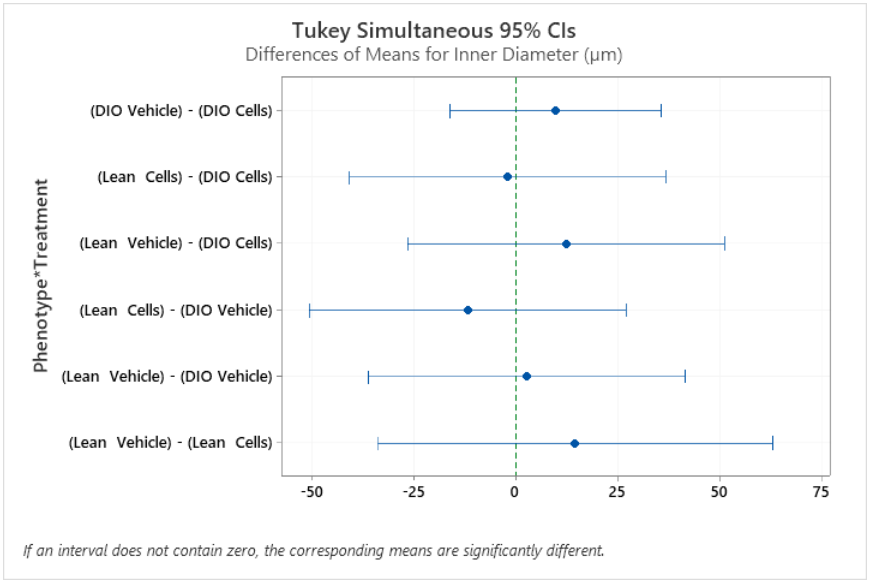

If an interval does not contain zero, the corresponding means are significantly different.

Comparisons between Wall Thickness of Operated and Sham Hindlimbs

Analysis: Tukey Pairwise and 2-sample T-test

Tukey Pairwise Comparisons: Hindlimb

Grouping Information Using the Tukey Method and 95% Confidence

Hindlimb	N	Mean	Grouping
Operated	18	13.0261	A
Sham	18	11.3365	A

Means that do not share a letter are significantly different.

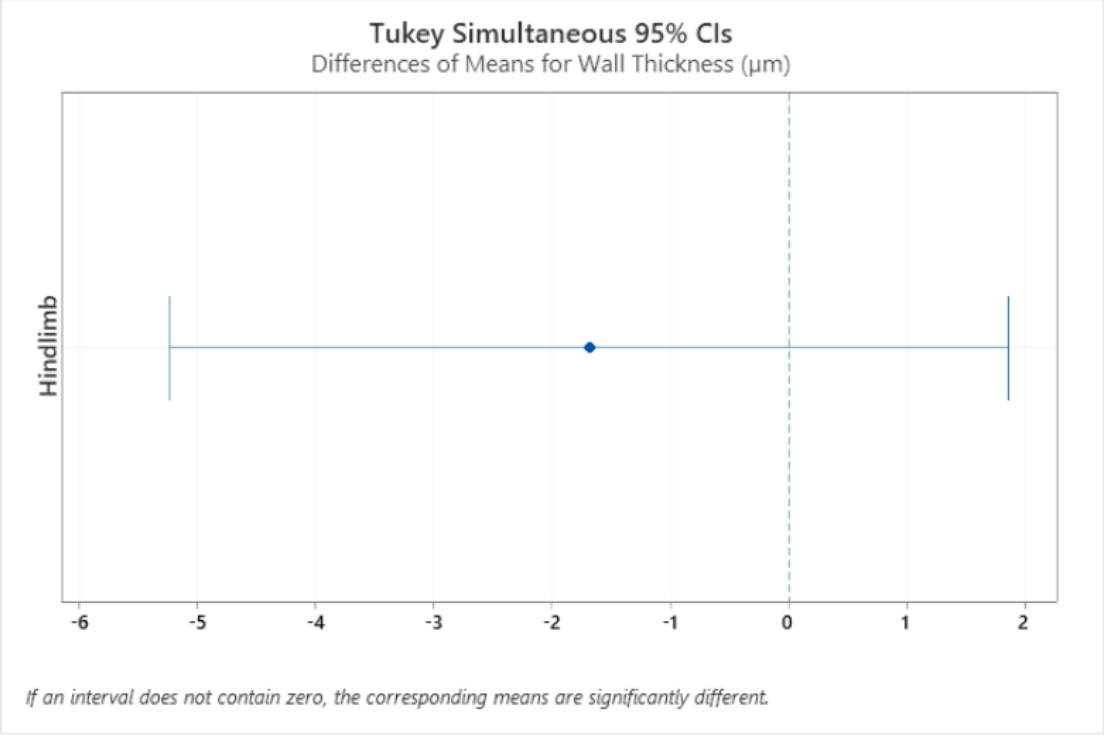

If an interval does not contain zero, the corresponding means are significantly different.

WALL THICKNESS

Two-Sample T-Test and CI: Wall Thickness (µm), Hindlimb

Method

μ_1: population mean of Wall Thickness (µm) when Hindlimb = Operated
μ_2: population mean of Wall Thickness (µm) when Hindlimb = Sham
Difference: $\mu_1 - \mu_2$

Equal variances are not assumed for this analysis.

Descriptive Statistics: Wall Thickness (µm)

Hindlimb	N	Mean	StDev	SE Mean
Operated	18	13.03	6.15	1.4
Sham	18	11.34	4.12	0.97

Estimation for Difference

Difference	95% CI for Difference
1.69	(-1.88, 5.26)

Test

Null hypothesis $H_0: \mu_1 - \mu_2 = 0$
Alternative hypothesis $H_1: \mu_1 - \mu_2 \neq 0$

T-Value	DF	P-Value
0.97	29	0.341

Comparisons between Wall Thickness of Phenotype (DIO v. Lean) and Treatment (Cells v. Vehicle)

Analysis: 2-way ANOVA and Tukey Pairwise

WALL THICKNESS

General Linear Model: Wall Thickness (µm) versus Phenotype, Treatment

Method

Factor coding (-1, 0, +1)

Factor Information

Factor	Type	Levels	Values
Phenotype	Fixed	2	DIO, Lean
Treatment	Fixed	2	Cells, Vehicle

Analysis of Variance

Source	DF	Adj SS	Adj MS	F-Value	P-Value
Phenotype	1	112.273	112.273	4.29	0.046
Treatment	1	0.412	0.412	0.02	0.901
Phenotype*Treatment	1	6.325	6.325	0.24	0.626
Error	32	836.863	26.152		
Total	35	956.286			

Model Summary

S	R-sq	R-sq(adj)	R-sq(pred)
5.11390	12.49%	4.28%	0.00%

Coefficients

Term	Coef	SE Coef	T-Value	P-Value	VIF
Constant	11.00	1.03	10.73	0.000	
Phenotype					
DIO	2.12	1.03	2.07	0.046	1.00
Treatment					
Cells	-0.13	1.03	-0.13	0.901	1.45
Phenotype*Treatment					
DIO Cells	0.50	1.03	0.49	0.626	1.45

Regression Equation

Wall Thickness (µm) = 11.00 + 2.12 Phenotype_DIO - 2.12 Phenotype_Lean
- 0.13 Treatment_Cells + 0.13 Treatment_Vehicle
+ 0.50 Phenotype*Treatment_DIO Cells - 0.50 Phenotype*Treatment_DIO
Vehicle - 0.50 Phenotype*Treatment_Lean Cells
+ 0.50 Phenotype*Treatment_Lean Vehicle

Fits and Diagnostics for Unusual Observations

Obs	Wall Thickness (µm)	Fit	Resid	Std Resid	
2	23.97	13.50	10.47	2.12	R

R Large residual

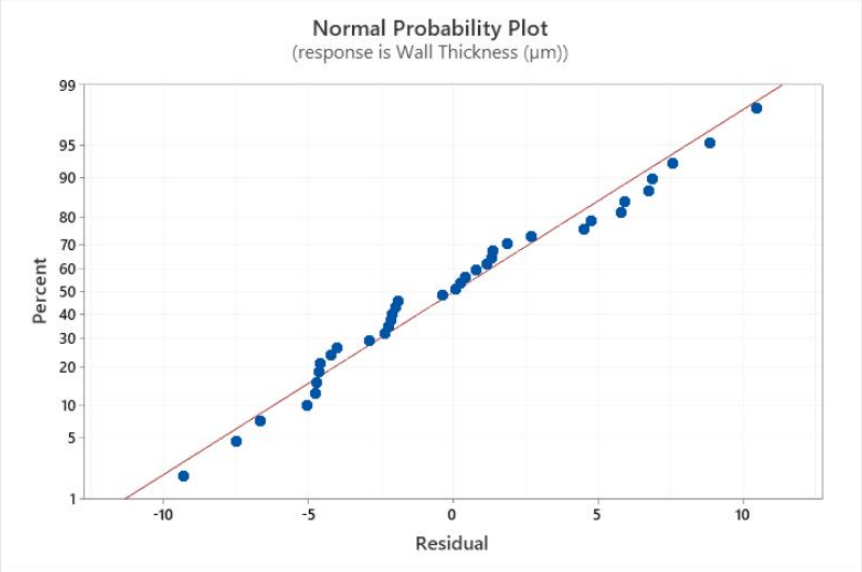
Normal Probability Plot
(response is Wall Thickness (µm))
Percent
99
95
90
80
70
60
50
40
30
20
10
5
1
-10
-5
0
5
10
Residual

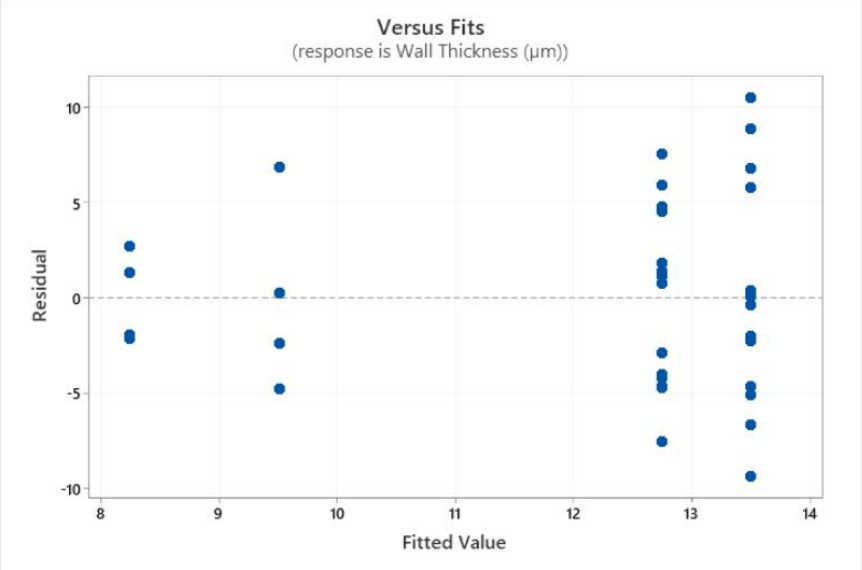
Versus Fits
(response is Wall Thickness (µm))
Residual
10
5
0
-5
-10
8
9
10
11
12
13
14
Fitted Value

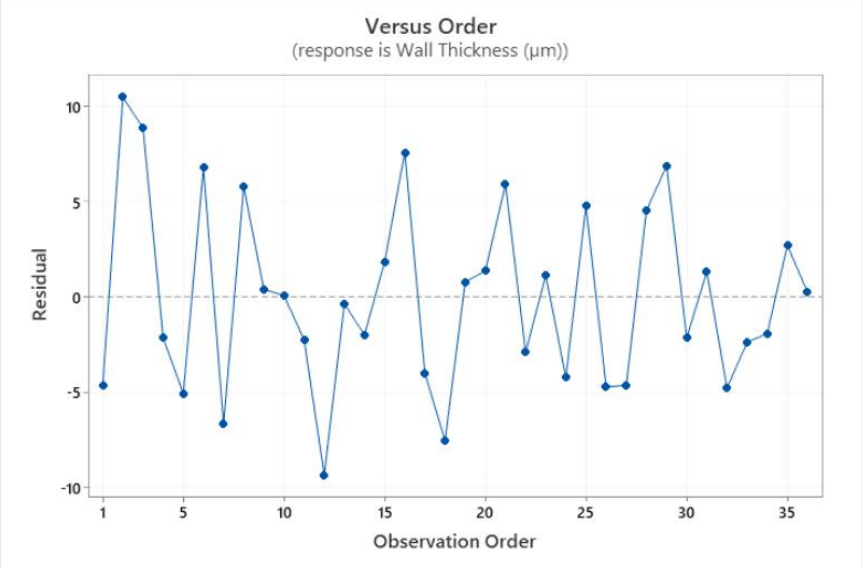
Versus Order
(response is Wall Thickness (µm))
Residual
10
5
0
-5
-10
1
5
10
15
20
25
30
35
Observation Order

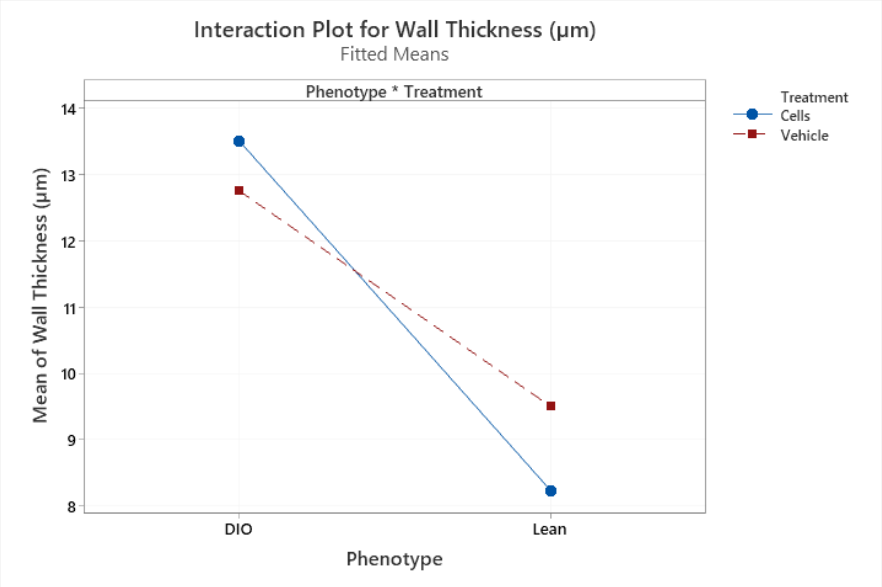

Tukey Pairwise Comparisons: Phenotype*Treatment

Grouping Information Using the Tukey Method and 95% Confidence

Phenotype*Treatment	N	Mean	Grouping
DIO Cells	14	13.5007	A
DIO Vehicle	14	12.7498	A
Lean Vehicle	4	9.5102	A
Lean Cells	4	8.2447	A

Means that do not share a letter are significantly different.

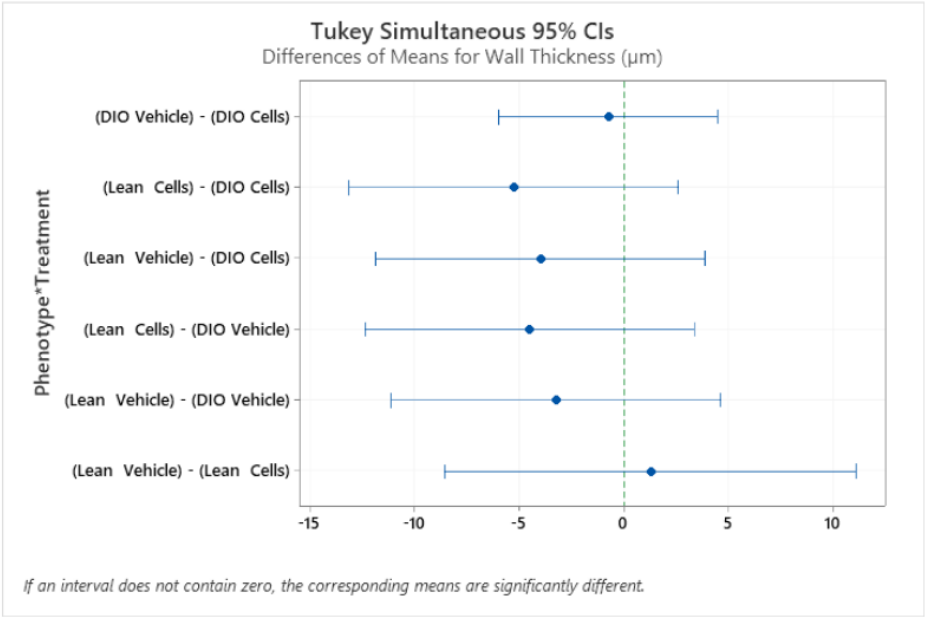

If an interval does not contain zero, the corresponding means are significantly different.